CAMBRIDGE
UNIVERSITY PRESS

Regular Article

Greater affective network maturity is associated with better clinical outcomes in women with early sexual trauma

Olena Kleshchova[1] (ORCID), Jack Grinband[2] and Mariann R. Weierich[1]

[1]Department of Psychology, University of Nevada Reno, Reno, NV, USA and [2]Departments of Psychiatry and Radiology, Columbia University, New York State Psychiatric Institute, New York, NY, USA

Abstract

Early-life adversity accelerates the maturation of affect-related circuitry, which might be a short-term adaptation with long-term tradeoffs. Sexual trauma is associated with a particularly strong impact on pubertal development and mental health outcomes. Our objective was to test the relations between trauma type, affective network maturity, and mental health outcomes in young women with trauma history. Trauma-exposed women aged 18–29 completed a clinical interview ($n = 35$) and an fMRI scan ($n = 28$). We used a public data set to train a machine learning algorithm to predict age from resting-state affective network connectivity and calculated network maturity as the difference between predicted and true age. We also performed principal component analysis on mental health outcomes and retained two components: clinical and state psychological outcomes. Compared to nonsexual trauma ($n = 17$), sexual trauma ($n = 11$) was associated with greater affective network maturity. In addition, for sexual trauma only, greater affective network maturity was associated with better clinical but not state psychological outcomes. These results suggest that sexual trauma during development might uniquely alter the maturational trajectory of affect-related circuitry, with distinct mental health consequences in emerging adulthood. Whereas delayed affective network maturation is associated with adverse clinical outcomes, accelerated affective network maturation might confer resilience in survivors.

Keywords: affective network; brain maturity; machine learning; resting functional connectivity; sexual trauma

Introduction

Traumatic stress during sensitive periods of development is a risk factor for mental health problems in adulthood (e.g., Green et al., 2010; Hoppen & Chalder, 2018). Compared to other types of adversity, early-life sexual trauma is associated with higher risk and symptom severity across a range of diagnostic domains, including posttraumatic stress disorder (PTSD), depression, anxiety, and substance use (e.g., Dworkin et al., 2017; Molnar et al., 2001; O'Brien et al., 2016). Disrupted brain development is a potential mechanism that might account for the relation between early-life trauma and adverse mental health outcomes (e.g., Andersen & Teicher, 2008; Bick & Nelson, 2016). Further, trauma type, and in particular sexual trauma, might moderate this relation by exerting circuit-specific effects on neurodevelopment (e.g., Cohodes et al., 2020).

Growing evidence suggests that early-life adversity accelerates development and sexual maturation, particularly in girls, as indexed by earlier pubertal onset (Gur et al., 2019), younger age at menarche (Colich et al., 2019), and accelerated cellular aging (e.g., Sumner et al., 2019). The developmental effects of early-life adversity depend on the type of adversity, such that threat-related

adversity (e.g., sexual abuse, violence) is associated with accelerated pubertal development and cellular aging, whereas deprivation-related adversity (e.g., neglect) is not (Colich et al., 2020). Compared to other trauma types, early-life sexual trauma appears to have an especially strong association with abnormally advanced pubertal development (e.g., Mendle et al., 2014, 2016; Noll et al., 2017). Accelerated maturation in turn predicts a range of mental health problems in adolescence, such as internalizing symptoms (Mendle et al., 2014), and mood, anxiety, and substance use disorders (e.g., Platt et al., 2017). Moreover, accelerated maturation, as indexed by earlier menarche and advanced cellular aging, mediates the relation between early-life adversity and later psychiatric symptoms (Colich et al., 2019; Sumner et al., 2019).

In addition to advancing pubertal development, early-life trauma might alter the developmental trajectory of brain maturation. For example, adolescent girls who have been exposed to childhood trauma (Gur et al., 2019) or physical neglect (Keding et al., 2021) show greater structural maturity of the brain as a whole compared to non-trauma-exposed peers. Furthermore, the relation between early-life adversity and greater structural brain maturity is particularly strong among adolescents exposed to threat-related adversity, such as sexual abuse, home violence, or emotional abuse (Drobinin et al., 2022). However, emerging longitudinal evidence points to complex and nonlinear effects of early-life adversity on neurodevelopment, such that initially accelerated brain maturation may be followed by delayed brain maturation later (Rakesh et al., 2021).

Cite this article: Kleshchova, O., Grinband, J., & Weierich, M. R. (2024). Greater affective network maturity is associated with better clinical outcomes in women with early sexual trauma. *Development and Psychopathology* **36**: 1458–1468, https://doi.org/10.1017/S0954579423000676

Check for updates

Although early-life adversity has been associated with accelerated global maturation of the brain as a whole, there is also growing evidence of circuit- and network-specific effects (e.g., Colich et al., 2020; Keding et al., 2021). Frontolimbic circuitry centered on the amygdala, hippocampus, and medial prefrontal cortex (mPFC) might be particularly susceptible to the neurodevelopmental effects of early-life adversity, given its role in affective processing, threat detection, and stress response regulation (VanTieghem & Tottenham, 2017). For example, early maternal separation and low maternal care accelerate the maturation of the hippocampus (e.g., Bath et al., 2016), amygdala (Ono et al., 2008), and frontolimbic circuits (Callaghan et al., 2014; Manzano Nieves et al., 2020) in non-human animals. Similarly, maternally deprived children have been shown to display a more mature pattern of amygdala-mPFC coupling during emotion processing (Gee et al., 2013) and at rest (Herzberg et al., 2021) compared to peer controls, although the reliability of this association and the use of task-based amygdala-mPFC coupling as an index of brain maturity has been called into question (Bloom et al., 2022; Colich et al., 2020) Childhood adversity also has been associated with accelerated structural maturation of the frontolimbic circuitry in adolescence, as indexed by lesser gray matter volumes, thinner cortex, greater white matter integrity, and greater longitudinal reductions in gray matter volume spanning prefrontal, insular, medial temporal, and subcortical limbic regions (e.g., Busso et al., 2017; Gur et al., 2019; Kelly et al., 2013; Tyborowska et al., 2018). In addition, early-life adversity has been associated with accelerated functional maturation of frontolimbic circuitry in young adolescents (Brieant et al., 2021; Thijssen et al., 2022). Furthermore, accelerated frontolimbic maturation has been specifically linked to threat-related adversity (Colich et al., 2020). Despite much evidence in support of accelerated maturation, some studies have shown delayed maturation of affective circuitry in trauma-exposed youths (e.g., Keding et al., 2021; Whittle et al., 2013). This apparent discrepancy in the literature might point to nonlinear effects of early-life adversity on the neurodevelopmental trajectory. For example, a recent longitudinal study showed that neighborhood disadvantage is associated with accelerated brain maturation in early adolescence followed by delayed maturation in late adolescence in at-risk youths (e.g., Rakesh et al., 2021).

Differences in the neurodevelopmental effects of early-life trauma (i.e., acceleration or delay) could also underlie different functional outcomes and thus reflect vulnerability or resilience. Earlier frontolimbic maturation has been proposed to have adaptative value in harsh early-life environments by promoting earlier emergence of affect-related functions and stress-regulatory behaviors (Callaghan & Tottenham, 2016). For example, accelerated limbic maturation is associated with earlier development of stress reactivity and fear learning in non-human animals (e.g., Bath et al., 2016; Callaghan et al., 2014). Similarly, a more mature pattern of amygdala-mPFC coupling during emotion processing has been associated with less separation anxiety in maternally deprived children (Gee et al., 2013), although recent research has not replicated this association in more normative samples (e.g., Bloom et al., 2022). Additionally, greater functional maturity of resting corticolimbic connectivity in adolescents has been shown to mediate the relation between early-life adversity and less internalizing symptoms two years later (Brieant et al., 2021). Consistent with the hypothesized adaptive value of accelerated maturation, delayed frontolimbic maturation has been associated with psychiatric symptoms (e.g., Albaugh et al., 2017; Ducharme

et al., 2014; Vanes et al., 2020), particularly in trauma-exposed youths (e.g., Keding et al., 2021; Whittle et al., 2013). Furthermore, slower development of frontal and limbic structures has been shown to mediate the relation between early-life adversity and poor outcomes in adolescents (e.g., Barch et al., 2022; Hanson et al., 2015; Whittle et al., 2016).

Accelerated pubertal development and frontolimbic maturation might constitute a short-term adaptation with long-term mental health consequences (e.g., Belsky and Shalev, 2016; Callaghan & Tottenham, 2016). For example, earlier pubertal onset has been associated with psychiatric symptoms in adolescence (e.g., Colich et al., 2019; Mendle et al., 2014; Platt et al., 2017). However, the precise relationship between altered development and short-term vs. long-term outcomes remains unclear given prior reports of both positive and negative mental health outcomes of accelerated maturation. One possibility is that negative outcomes of early-life trauma might be mediated by accelerated sexual maturation and biological aging (e.g., Colich et al., 2019; Sumner et al., 2019), whereas positive outcomes might be mediated by selectively accelerated maturation of neural circuitry involved in affective processing and stress regulation (e.g., Brieant et al., 2021). An alternative explanation supported by emerging evidence suggests that the mental health tradeoffs of accelerated brain maturation in early adolescence might result from a subsequent deceleration of brain maturation in late adolescence (e.g., Rakesh et al., 2021). For example, a prospective study of youths with a family history of mood disorders showed that the risk of developing a mood disorder was associated with delayed brain maturation during late adolescence and emerging adulthood (de Nooij et al., 2020).

Affect-related frontolimbic circuits follow protracted maturational trajectories well into adulthood, as indexed by age-related changes in synaptic density (Petanjek et al., 2011), subcortical gray matter volume (Narvacan et al., 2017), white matter structure (Lebel et al., 2012), intracortical myelination (Grydeland et al., 2013), and functional connectivity (Gabard-Durnam et al., 2014). Due to this prolonged immaturity and a high concentration of receptors for various stress mediators (e.g., Joëls & Baram, 2009), frontolimbic circuitry might be particularly sensitive to traumatic stress not only in childhood and adolescence but also in early adulthood. However, as research on posttrauma maturation of affect-related circuitry beyond childhood and adolescence is still lacking, the relation between altered frontolimbic development and later mental health outcomes remains unclear.

The importance of clarifying the relation between trauma-related alterations in frontolimbic maturity and mental health outcomes in emerging adults is threefold. First, studies that focus on trauma-exposed children and adolescents miss the delayed effects of early-life trauma on mental health, including adult-onset psychopathology (e.g., Green et al., 2010). Conversely, assessment of mental health outcomes in young adulthood permits stronger conclusions about vulnerability vs. resilience to adverse outcomes of early-life trauma. Second, because frontolimbic circuits remain malleable into early adulthood (e.g., Petanjek et al., 2011), temporary deviations from normative maturity in childhood or adolescence that eventually normalize are unlikely to account for adverse mental health outcomes in adulthood. Finally, emerging research suggests that the neurodevelopmental alterations of early-life trauma and their functional significance are age-dependent (Rakesh et al., 2021), such that potentially beneficial early acceleration might be followed by potentially detrimental late deceleration of maturation. Thus, it is important to characterize

the trauma-related effects on brain maturation in emerging adulthood separately from earlier stages of development.

Trauma exposure during sensitive periods of frontolimbic development might interact with the maturational trajectories of affect-related circuits to produce distinct mental health outcomes later in life (e.g., Gee & Casey, 2015). Of the various types of childhood adversity, sexual trauma has been robustly associated with stronger impact on pubertal maturation (e.g., Noll et al., 2017) and poorer mental health outcomes (e.g., Dworkin et al., 2017), however the effect of sexual trauma on the maturation of affect-related circuitry remains unclear. Early-life sexual trauma is thought to be distinct from other trauma types in that it represents a particularly damaging combination of traumatic sexualization, betrayal, powerlessness, and stigmatization (Finkelhor & Browne, 1985), which together exert profound effects on survivors' affective function and emotion regulation abilities. Emotion dysregulation in turn mediates the relation between sexual trauma and psychopathology (e.g., Raudales et al., 2019). Given the particular vulnerability associated with early-life sexual trauma, the impact of trauma on the maturation of affect-related circuitry might be especially pronounced in survivors of sexual trauma compared to other types of adversity and might account for vulnerability or resilience to adverse mental health outcomes.

To investigate this question, we used a machine-learning-based approach to measuring functional maturity of affect-related brain circuits. Our first objective was to test differences in the functional maturity of affective networks in young women who had been exposed to either sexual or nonsexual trauma prior to study enrollment (i.e., during childhood, adolescence, or emerging adulthood), which we refer to as early-life trauma. Given the absence of a universally accepted definition of "early life" and the growing evidence of protracted brain maturation well into young adulthood (e.g., Grydeland et al., 2013; Lebel et al., 2012), here we define early-life trauma as traumatic stress during the first three decades of life when the brain continues to undergo structural and functional maturation. Our second objective was to quantify the relation between affective network maturity and trauma-related mental health outcomes in emerging adulthood. We used a public neuroimaging data set of healthy no-trauma controls ages 6–45 to train a machine learning algorithm to predict age based on resting-state connectivity of affect-related networks (orbito-affective and cingulo-opercular). We then used the trained algorithm to predict age from functional affective network connectivity in a separate sample of trauma-exposed women ages 18–29 with a history of either sexual or nonsexual trauma.

We hypothesized that, compared to nonsexual trauma, sexual trauma would be associated with greater functional affective network maturity, as indexed by greater difference between predicted age and true age. Such a result would be consistent with accelerated frontolimbic maturation following early-life sexual trauma. Given the well-documented differences in the maturational trajectories of different brain circuits (e.g., Grydeland et al., 2013; Lebel et al., 2012), the calculated discrepancy between predicted and true age should not be interpreted as an index of *global brain* maturity, but rather as an index of *network-specific* maturity (i.e., the functional maturity of affect-related circuitry). We also hypothesized that affective network maturity would be associated with mental health outcomes, which we derived by performing dimensionality reduction on eight measures of trauma-related outcomes. A negative association between affective network maturity and adverse outcomes would suggest that greater affective network maturity has adaptive value even in emerging

adulthood. Conversely, a positive association would be consistent with mental health tradeoffs of accelerated affective network maturation. Finally, we hypothesized that trauma type would moderate the relation between affective network maturity and mental health outcomes, such that the association between affective network maturity and outcomes would be more pronounced in participants with sexual vs. nonsexual trauma.

Materials and methods

Participants

We recruited 36 trauma-exposed women ages 18–29 ($M = 21.2$, $SD = 2.7$) from an urban university in the northeastern United States based on their responses to the Life Events Checklist, a self-report screen for potential trauma exposure (Gray et al., 2004). We verified trauma exposure during a structured clinical interview. Participants were excluded if they had a history of head trauma, had a history of a developmental or neurological disorder, or had MRI contraindications.

Procedure

Participants completed two study sessions: a lab visit, which included a clinical interview and questionnaires, and an MRI scan. The study protocol was approved by the Institutional Review Board and conducted in accordance with the Code of Ethics of the World Medical Association (Declaration of Helsinki).

Clinical interview

Following informed consent, participants completed a clinical interview that included the Clinician-Administered PTSD Scale (CAPS-5; Weathers et al., 2018) and the Structured Clinical Interview for DSM-IV Disorders (SCID; First et al., 2002a). We used the CAPS to assess trauma exposure and PTSD symptoms and the SCID to assess lifetime history of major psychiatric disorders. Trauma exposure was defined according to Criterion A of the CAPS.

Questionnaires

After the interview, participants completed "state" psychological measures; although the timeframe for each measure varied slightly, we conceptualized the responses to each to reflect the participant's general state during participation, and we distinguished between these phenomena and clinical outcomes. The measures were the Perceived Stress Scale (PSS, Cohen et al., 1983), the Beck Depression Inventory II (BDI-II, Beck et al., 1996), the State-Trait Anxiety Inventory-State Version (STAI-S, Spielberger et al., 1983), and the Positive and Negative Affect Schedule (PANAS, Watson et al., 1988). The PSS is a 10-item measure of the degree to which life events over the past month are perceived as stressful, uncontrollable, and unpredictable. The BDI-II is a 21-item measure of depressed mood over the past two weeks. The STAI-S is a 20-item measure of state anxiety. The PANAS is a 20-item measure of state negative and positive affect.

MRI scan

The MRI session included 13 minutes of structural scans followed by a 7-min resting scan during which the participants were instructed to fixate on a white cross on a black background and let their minds wander. Imaging data were acquired on a Siemens MAGNETOM Prisma 3T MRI scanner using a 64-channel gradient head coil. We acquired T1-weighted (T1w) images using

the MPRAGE sequence (TR/TE/flip angle = 2.4 s/2.28 ms/8°; FOV = 256 × 256 mm; voxel size = 0.8 mm^3) and resting-state functional data using multiband image acquisition and a gradient-echo echo-planar imaging T2*-weighted sequence (TR/TE/flip angle = 995 ms/34 ms/52°; FOV = 208 × 208 mm; voxel size = 2 mm^3; MB = 6; 425 volumes).

Training data set for machine learning

To build a normative model of affective network maturation, we used the enhanced Nathan Kline Institute-Rockland Sample (NKI-RS; Nooner et al., 2012) as the training data set for machine learning. Our goal was to build a sex-specific normative model of functional maturation of the affective networks from middle childhood through middle adulthood in the absence of prior trauma exposure or clinical history. To this end, we selected the normative sample using the following inclusion criteria: female, age 6–45, right-handed, no neurological, developmental, or psychiatric disorders, and no prior history of trauma. These stringent selection criteria were used to minimize known sources of variability in functional connectivity that are unrelated to age, such as sex, handedness, psychiatric history, and trauma exposure. Our choice of a wider age range for the training data set compared to the test data set was motivated by both conceptual and practical considerations. First, because the degree of the hypothesized maturation acceleration or delay was unclear, we chose relatively wide "safety margins" (±12–16 years) to avoid underestimating any deviations from the normative trajectory. In addition, our wide age range was meant to increase the model's prediction accuracy for the age group of interest (age 18–29) by exposing the machine learning algorithm to relative extremes of the brain age spectrum relative to the age group of interest (i.e., middle childhood and middle adulthood). Finally, by including a wider age range, we were able to not only increase the sample size but also increase age-related variability while decreasing age-unrelated variability through stringent exclusion criteria.

Clinical history. In the NKI-RS sample, trauma history was assessed using the University of California at Los Angeles Posttraumatic Stress Disorder Reaction Index (Pynoos et al., 1998). Lifetime neurological and psychiatric history was assessed using the Structured Clinical Interview for DSM-IV-TR (First et al., 2002b) and the Adult ADHD Clinical Diagnostic Scale (Kessler et al., 2010) for participants above age 17 and the Kiddie Schedule for Affective Disorders and Schizophrenia for participants under age 18 (Kaufman et al., 1997).

Neuroimaging data. NKI-RS imaging data were acquired on a Siemens MAGNETOM Trio Tim 3T MRI scanner using a 32-channel gradient head coil. We used the selected participants' T1w MPRAGE images (TR/TE/flip angle = 1.9 s/2.52 ms/9°; FOV = 250 × 250 mm; voxel size = 1 mm^3) and the 9.5-min resting-state scans which were acquired using multiband image acquisition and a gradient-echo echo-planar imaging T2*-weighted sequence (TR/TE/flip angle = 1.4 s/30 ms/65°; FOV = 224 × 224 mm; voxel size = 2 mm^3; MB = 4; 404 volumes). During the resting scan, NKI-RS participants were instructed to fixate on a white cross on a black background.

Data preparation

Neuroimaging data preprocessing

Usable MRI data were available for 85 healthy no-trauma controls in the training data set (NKI-RS sample) and 29 trauma-exposed participants in the test data set. The training and test data sets had

comparable neuroimaging parameters and therefore were pre-processed similarly (see Supplementary Information, SI). Briefly, anatomical and functional scans were preprocessed using fMRIPrep (Esteban et al., 2019) and converted to the Connectivity Informatics Technology Initiative format using the fmriprep_ciftify BIDS-app (Dickie et al., 2019). All subsequent denoising operations and analyses were performed on the preprocessed Connectivity Informatics Technology Initiative data.

Denoising of resting-state functional data

To minimize the influence of head motion on estimates of functional connectivity and brain maturity, we excluded high-motion participants and performed nuisance regression and high-pass filtering (see SI). After exclusion of 6 high-motion participants from the training data set (see SI for exclusion criteria), the final sample included 79 participants (age 6–45, $M = 23.2$, $SD = 11.8$). No participants were excluded from the test data set.

Functional connectivity estimation

All functional connectivity estimation operations were performed on the cleaned and filtered functional data using Connectome Workbench and custom Matlab code (see SI). Briefly, we used the Cole-Anticevic Brain-wide Network Partition (Ji et al., 2019) to parcellate the brain into 718 regions of interest (ROIs) and excluded ROIs with group median temporal signal-to-noise ratio of <100. We calculated correlation coefficients between mean time series from each pair of the remaining 567 ROIs and performed Fisher's r-to-Z transformation. To minimize the effects of residual motion on functional connectivity, we excluded edges that were correlated with head motion at uncorrected $p < .05$ (39%) from all subsequent analyses. The features that were used to train the final model are presented in SI.

Data analysis

Affective network maturity estimation

All machine learning operations were performed in Matlab R2019b using the Statistics and Machine Learning Toolbox and the Regression Learner App. We used support vector regression (SVR; Smola and Schölkopf, 2004; Vapnik, 1995) to train the normative model of affective network maturation using the selected NKI-RS participants as the training data set (Dosenbach et al., 2010; Nielsen et al., 2019) and the trauma-exposed participants as the test data set (see SI for details). Briefly, the affective network maturation model was trained on 500 features sampled from the cingulo-opercular and orbito-affective networks (Ji et al., 2019) based on the strength of their correlations with age. We performed leave-one-out cross-validation on the training sample to determine the accuracy of the trained SVR model and used permutation testing to determine whether the model's performance was statistically different from chance. We then used the trained SVR model to predict the ages of trauma-exposed participants and calculated affective network maturity as the difference between predicted age and true chronological age.

The trained SVR model showed high accuracy ($R^2 = .86$, $r = .93$, RMSE = 4.6, MAE = 3.8) and was statistically significant at $p < .001$ in the training data set (Figure 1). The MAE for the test group as a whole was 2.5. The performance of our model is consistent with reported model performances in previous life span studies that used a range of machine learning algorithms to predict age based on various neuroimaging modalities and feature sets (Franke et al., 2020). Although most prior studies used training
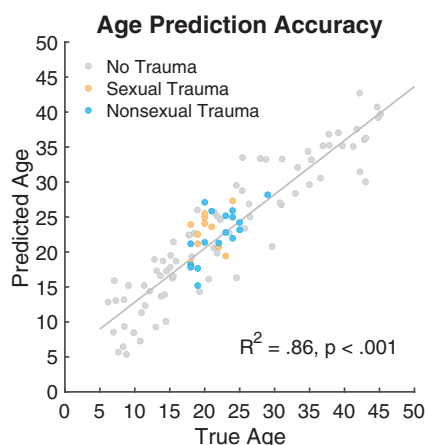
Figure 1. Performance of the machine learning algorithm trained to predict age based on affective network connectivity (MAE = 3.8, RMSE = 4.6, R^2 = .86, r = .93, $p < .001$). Linear support vector regression was trained on 500 features sampled from the cingulo-opercular and orbito-affective networks ("affective networks") based on the strength of their correlations with age. Affective network maturity was calculated as the difference between predicted age and true age (i.e., prediction errors).

data sets ranging from $n = 122$ ($R^2 = .57$; age range: 7–31; Nielsen et al., 2019) to $n = 2354$ ($R^2 = .87$; age range: 19–82; Liem et al., 2017), successful "brain age" prediction has been achieved with as few as 74 participants ($R^2 = .46$; age range 8–18: Keding et al., 2021), 63 participants ($R^2 = .61$; age range 18–45: Tian et al., 2016), or even 44 participants ($R^2 = .48$; age range: 23–74; Neeb et al., 2006) in the training data set. Despite our relatively small training data set, our trained model showed better performance compared to previous studies that used resting-state fMRI to predict age in more heterogenous mixed-gender samples and achieved R^2 in the range of .55–.61 (Dosenbach et al., 2010; Nielsen et al., 2019; Tian et al., 2016).

We did not perform bias correction associated with regression to the mean, because prediction errors were not correlated with chronological age, $r = -.33$, $p = .087$, and because bias correction is inaccurate when the age ranges of the training and test samples are different, such as in our case (Liang et al., 2019). To test the degree to which regression to the mean may have influenced our results, we repeated our analyses of affective network maturity with chronological age as a covariate. Chronological age did not improve model fit and was not a statistically significant predictor.

Principal component analysis on mental health outcomes

To generate summary indices of mental health outcomes in trauma-exposed women, we performed dimensionality reduction on eight measures of psychological functioning and past and current clinical history. To estimate the amount of shared variance among different measures of mental health outcomes, we calculated Pearson's correlations between perceived stress (PSS), depressed mood (BDI), state anxiety (STAI), negative affect (PANAS), PTSD symptom number and severity (CAPS), and number of current and past psychiatric diagnoses (SCID). The predominance of strong positive correlations among measures of mental health outcomes (Figure 2A) reflected a substantial amount of shared variance and warranted dimensionality reduction. We performed principal component analysis on the eight measures of mental health outcomes and retained the first two principal components with eigenvalues above 1, which together explained 72% of total variance (Figure 2B). After varimax rotation,

self-reported "state" measures of perceived stress, depressed mood, anxiety, and negative affect loaded most strongly on the first rotated component (PC1), whereas number of current and past psychiatric diagnoses loaded most strongly on the second rotated component (PC2). Number and severity of PTSD symptoms loaded moderately on both components (Figure 2C). For each participant, we calculated individual PC1 scores ("state psychological outcomes") and PC2 scores ("clinical outcomes"), which we used as two composite measures of mental health outcomes.

Associations between trauma type, affective network maturity, and mental health outcomes

To determine the effect of trauma type on mental health outcomes, we tested group differences in PC1 scores ("state psychological outcomes") and PC2 scores ("clinical outcomes") between participants with sexual vs. nonsexual trauma. To determine the effect of trauma type on affective network development, we tested group differences in affective network maturity (age prediction errors) between participants with sexual vs. nonsexual trauma. To clarify the functional significance of affective network maturity, we tested associations between affective network maturity (age prediction errors) and mental health outcomes (PC1 and PC2 scores). Finally, we tested trauma type as a moderator of the relations between mental health outcomes and affective network maturity. To minimize the influence of any outliers, we used a robust general linear model with the bisquare weight function to test all associations and group differences. All statistical analyses were performed using Matlab R2019b and the Statistics and Machine Learning Toolbox.

Results

Descriptive data

Participant information is presented in Table 1. Thirteen participants (37%) endorsed sexual violence as their index trauma, 11 of whom had usable fMRI data. Twenty-two participants endorsed nonsexual trauma as their index trauma, 17 of whom had usable fMRI data. One participant did not provide the details of her trauma and was excluded from the analysis. Age at the earliest trauma ranged from 3 to 27 years, and time since the most recent trauma ranged from less than a year to 15 years. Participants with sexual vs. nonsexual trauma did not differ in age, Wilcoxon rank-sum test: $Z = 0.81$, $p = .418$, $r = .14$; number of traumatic events, $Z = 0.15$, $p = .883$, $r = .02$; age at the earliest trauma, $Z = 1.47$, $p = .141$, $r = .25$; or time since the most recent trauma, $Z = 0.86$, $p = .389$, $r = .15$.

Participants with sexual vs. nonsexual trauma did not differ in perceived stress, $Z = 0.86$, $p = .392$, $r = .14$; depressed mood, $Z = 0.79$, $p = .432$, $r = .13$; negative state affect, $Z = 0.55$, $p = .583$, $r = .09$; or positive state affect, $Z = -1.06$, $p = .288$, $r = -.18$. However, participants with sexual vs. nonsexual trauma showed a nonsignificant trend (medium effect size) towards greater state anxiety, $Z = 1.90$, $p = .058$, $r = .32$. Almost half (46%) of the participants with sexual trauma met criteria for a provisional PTSD diagnosis compared to almost one-third (27%) of the participants with nonsexual trauma. Although there was no difference in probability of a provisional PTSD diagnosis by trauma type, $\chi^2 = 1.29$, $p = .256$, participants with sexual trauma endorsed more, $Z = 2.87$, $p = .004$, $r = .48$, and more severe, $Z = 2.00$, $p = .045$, $r = .34$, PTSD symptoms compared to participants with nonsexual trauma. There were no differences by trauma type in number of current psychiatric diagnoses, $Z = 0.74$, $p = .462$,
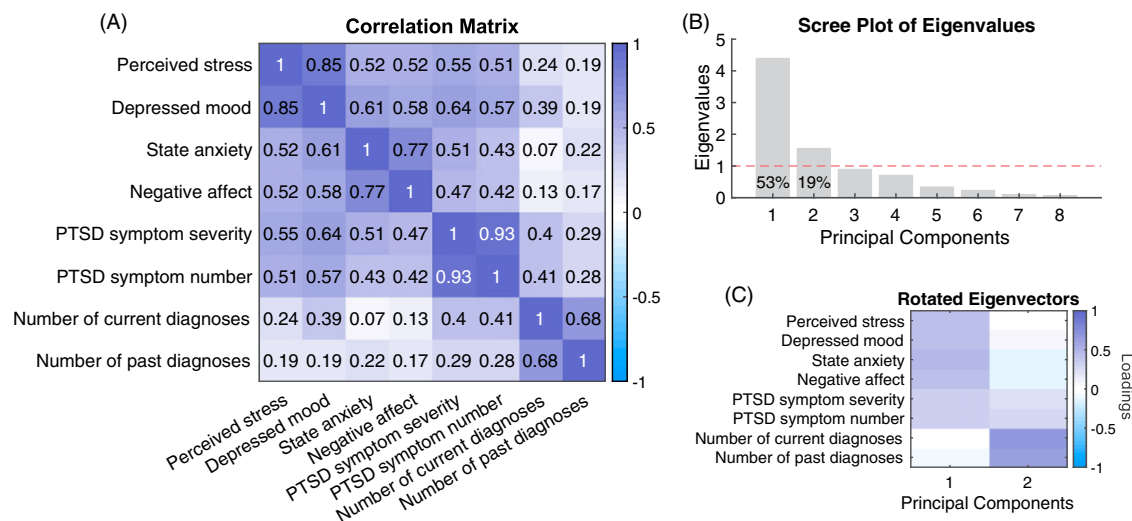
Figure 2. Principal component analysis on indices of mental health outcomes. Panel A: The high number of strong positive correlations among indices of mental health outcomes warranted dimensionality reduction. Panel B: The first two principal components together captured 72% of total variance. Panel C: The pattern of loadings of the original measures of mental health outcomes on the first two components after varimax rotation suggests that PC1 captures state psychological outcomes, whereas PC2 captures clinical outcomes.

$r = .12$, or past psychiatric diagnoses, $Z = 0.14$, $p = .888$, $r = .02$. We repeated the above analyses in participants with imaging data and obtained a similar pattern of results, except the probability of a provisional PTSD diagnosis was now higher in the sexual trauma group, $\chi^2 = 4.04$, $p = .044$.

Participants with sexual trauma showed a nonsignificant trend towards poorer state psychological outcomes indexed by PC1 scores, compared to participants with nonsexual trauma, $F(1,33) = 3.49$, $p = .071$, $R^2 = .10$ (Figure 3). There was no group difference by trauma type in clinical outcomes indexed by PC2 scores, $F(1,33) = 0.84$, $p = .365$, $R^2 = .03$.

Trauma type, affective network maturity, and mental health outcomes

Participants with sexual trauma showed greater affective network maturity indexed by age prediction errors ($M = 2.5$, $SD = 2.9$, range: -3.6 to 5.9), compared to participants with nonsexual trauma ($M = 0.6$, $SD = 2.7$, range: -3.8 to 7.1), $F(1,26) = 5.33$, $p = .029$, $R^2 = .17$ (Figure 4A). Affective network maturity was not associated with either state psychological outcomes indexed by PC1 scores, $F(1,26) = 0.41$, $p = .529$, $R^2 = .02$, or with clinical outcomes indexed by PC2 scores, $F(1,26) = 0.63$, $p = .433$, $R^2 = .03$. However, trauma type moderated the relation between clinical outcomes (independent variable) and affective network maturity (dependent variable), $F(1,24) = 4.44$, $p = .046$, $\eta_p^2 = .16$. Poorer clinical outcomes were associated with less affective network maturity in participants with sexual trauma but not in participants with nonsexual trauma (Figure 4B). Trauma type did not moderate the relation between psychological outcomes and affective network maturity, $F(1,24) = 0.21$, $p = .648$, $\eta_p^2 = .01$.

Discussion

In this proof-of-concept study, we used a machine learning approach to test atypical functional maturation of affect-related brain circuitry as a candidate mechanism that might account for the relation between exposure to early sexual trauma and adverse mental health outcomes in adulthood. Our first objective was to

compare the functional maturity of affective networks in young women who were exposed to either sexual or nonsexual trauma during formative years of brain development (i.e., early-life sexual trauma). Consistent with our hypothesis, young women with early sexual trauma showed greater affective network maturity compared to women with nonsexual trauma. This result aligns with the previously documented relation between early-life adversity and accelerated maturation of affect-related frontolimbic circuitry (e.g., Colich et al., 2020; Gur et al., 2019; Thijssen et al., 2022; Tyborowska et al., 2018). However, our data also suggest that the effect of early traumatic stress on neurodevelopment depends on the type of trauma. In line with previous evidence that sexual trauma is uniquely capable of advancing pubertal development (e.g., Mendle et al., 2016; Noll et al., 2017), our results suggest that sexual trauma also has a greater impact on frontolimbic maturation compared to other trauma types. These data also extend prior research in children and adolescents and show that the neurodevelopmental effects of traumatic stress are evident even in emerging adulthood, which is consistent with the protracted maturational trajectory of affect-related circuitry (e.g., Lebel et al., 2012; Narvacan et al., 2017). Together with prior literature, our results suggest that the developmental trajectory of affect-related circuitry remains sensitive to traumatic stress into emerging adulthood, and the effects of sexual trauma on affective network maturation can manifest beyond childhood and adolescence.

Our second objective was to test the functional significance of affective network maturity in relation to mental health outcomes in emerging adulthood. Counter to our hypothesis, affective network maturity was not associated with either state psychological or clinical outcomes in trauma-exposed women as a group. However, trauma type moderated the relation between affective network maturity and clinical outcomes. In women with sexual trauma, lesser affective network maturity was associated with poorer clinical outcomes, whereas there was no such relation in women with nonsexual trauma. In contrast, state psychological outcomes were not associated with affective network maturity in the trauma-exposed sample as a whole or in either trauma group separately. These results suggest that different types of trauma-related

Table 1. Participants

Variable	Sexual trauma (*n* = 13) Mean/*n*	SD/%	Nonsexual trauma (*n* = 22) Mean/*n*	SD/%
Demographics				
Age in years, *M, SD*	20.5	1.9	21.5	3.0
Race/ethnicity, *n*, %				
Asian/Pacific Islander	4.0	30.8	6.0	27.3
Black, non-Hispanic	3.0	23.1	3.0	13.6
Hispanic	2.0	15.4	9.0	40.9
White, non-Hispanic	3.0	23.1	3.0	13.6
Multiple	1.0	7.7	1.0	4.5
Trauma characteristics				
Number of traumatic events, *M, SD*	1.9	0.9	1.9	1.2
Earliest trauma before age 12, *n*, %	8.0	61.5	12.0	54.6
Earliest trauma at age 12–17, *n*, %	4.0	30.8	3.0	13.6
Earliest trauma after age 17, *n*, %	1.0	7.7	7.0	31.8
Age at first trauma, *M, SD*	9.2	5.1	12.7	6.9
Years since the most recent trauma, *M, SD*	4.6	4.3	3.2	3.3
Mental health outcomes				
Perceived Stress (PSS), *M, SD*	23.3	8.0	21.6	7.0
State anxiety (STAI-S), *M, SD*	53.3[†]	13.1	44.9	10.6
Depressed mood (BDI-II), *M, SD*	19.3	10.7	16.8	10.2
Negative state affect (PANAS), *M, SD*	10.1	4.1	9.1	3.0
Positive state affect (PANAS), *M, SD*	10.4	4.1	11.8	3.3
Total PTSD symptom count, *M, SD*	8.5**	3.5	4.6	4.5
Reexperiencing symptom count	1.9	1.5	1.4	1.6
Avoidance symptom count	1.3	0.8	0.8	0.8
NACM symptom count	3.2	1.1	1.6	1.7
Arousal symptom count	2.1	1.5	0.9	1.3
Total PTSD symptom severity, *M, SD*	21.3*	9.6	13.8	12.3
Reexperiencing symptom severity	4.5	3.2	3.7	3.5
Avoidance symptom severity	3.2	2.2	2.2	1.7
NACM symptom severity	7.9	3.0	4.8	4.8
Arousal symptom severity	5.7	4.0	3.1	3.3
Current PTSD diagnosis, *n*, %	6.0	46.2	6.0	27.3
Current psychiatric diagnosis[a], *n*, %	6.0	46.2	12.0	54.6
Past psychiatric diagnosis[a], *n*, %	8.0	61.5	15.0	68.2
Number of current psychiatric diagnoses[a], *M, SD*	0.7	1.0	1.3	1.8
Number of past psychiatric diagnoses[a], *M, SD*	1.8	2.0	1.9	2.0

Note. PSS = Perceived Stress Scale; STAI-S = State-Trait Anxiety Inventory-State Version; BDI-II = Beck Depression Inventory II; PANAS = Positive and Negative Affect Schedule; NACM = negative alterations in cognitions and mood.
[a]Any major psychiatric diagnosis other than PTSD, as assessed using the SCID.
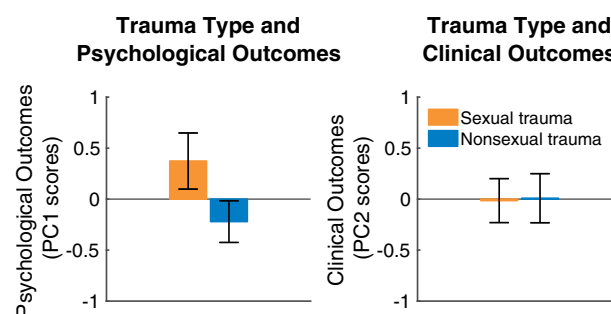[†]*p* < 0.1; *p* < 0.05; **p* < 0.01.

Figure 3. Trauma type and mental health outcomes. Compared to participants with a history of nonsexual trauma, participants with a history of sexual trauma showed a nonsignificant trend towards poorer state psychological outcomes indexed by PC1 scores (left panel) but no difference in clinical outcomes indexed by PC2 scores (right panel). Bars represent group means; error bars represent standard errors.

outcomes (i.e., state psychological vs. clinical) are mediated by different mechanisms and that subclinical levels of psychological distress are unrelated to the maturation of affect-related circuitry in early-trauma survivors.

The relation between greater affective network maturity and better clinical outcomes in sexual trauma survivors is consistent with the stress acceleration theory, which posits that accelerated maturation of affect-related circuitry is adaptive under conditions of early adversity (e.g., Callaghan & Tottenham, 2016). Our results suggest that greater maturity of affect-related circuitry might reflect resilience or constitute a protective factor against adverse clinical outcomes in survivors of early-life sexual trauma. This result is consistent with prior evidence of greater frontolimbic maturity being protective against internalizing symptoms in adolescents with early-life adversity (e.g., Brieant et al., 2021). In addition, given the robust literature documenting poorer clinical outcomes overall in sexual trauma survivors (e.g., Dworkin et al., 2017; O'Brien et al., 2016), the absence of a difference in clinical outcomes by trauma type might reflect a high prevalence of resilience in our sexual trauma group. This absence might be accounted for by greater affective network maturity in our sample of sexual trauma survivors.

Whereas accelerated affective network maturation might be adaptive, failure to accelerate maturation of affect-related circuitry following early sexual trauma might reflect a lack of adaptation, which might in turn confer vulnerability to adverse clinical outcomes. This interpretation is broadly consistent with previous evidence that delayed frontolimbic maturation is associated with psychiatric symptoms in adolescence (e.g., Albaugh et al., 2017; Ducharme et al., 2014; Keding et al., 2021; Vanes et al., 2020) and that slower development of frontal and limbic structures mediates the relation between early-life adversity and negative outcomes (e.g., Barch et al., 2022; Hanson et al., 2015; Whittle et al., 2016). Our results are consistent with prior literature and suggest that early-life trauma can alter frontolimbic development, however we also demonstrate that deviation from the normative maturational trajectory is not necessarily pathological and might reflect a compensatory developmental process that is necessary for successful adaptation following trauma.

Our results are consistent with the hypothesis that delayed maturation of the affect-related circuitry leads to higher risk of
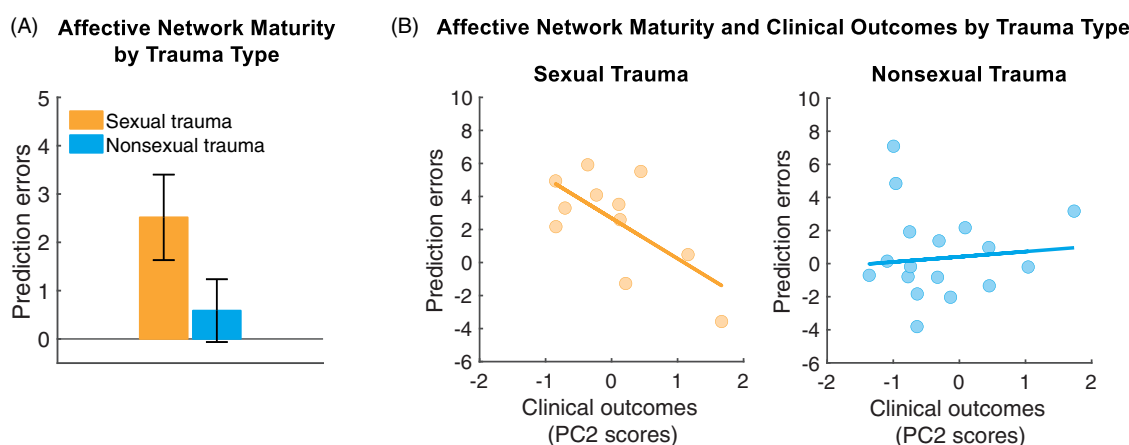
Figure 4. Trauma type, affective network maturity, and clinical outcomes. Panel A: Compared to participants with a history of nonsexual trauma, participants with a history of sexual trauma showed greater affective network maturity indexed by age prediction errors. Panel B: Trauma type moderated the relation between affective network maturity and clinical outcomes indexed by PC2 scores. Less affective network maturity was associated with poorer clinical outcomes in participants with sexual trauma but not in participants with nonsexual trauma. Bars represent group means; error bars represent standard errors. The lines of best fit were generated using robust regression.

adverse clinical outcomes in adults with early sexual trauma. However, the limitations of this study, such as the small sample size and cross-sectional design, preclude us from making strong claims about causal relations between sexual trauma, brain maturation, and clinical outcomes. Our data suggest that exposure to early-life sexual trauma accelerates functional maturation of affect-related networks. However, due to the cross-sectional nature of our study and our focus on emerging adults, we cannot determine whether this deviation from the normative maturational trajectory occurs shortly following trauma or later in development due to sleeper effects (e.g., Rakesh et al., 2021). In addition, because we measured brain maturity only once in emerging adulthood, we cannot assume that the observed direction or functional significance of accelerated maturation is the same at earlier stages of development. For example, risk of depression has been linked to greater global brain maturity in younger adolescents (Drobinin et al., 2022) and delayed brain maturation in older adolescents and emerging adults (de Nooij et al., 2020). Similarly, although we show that greater functional maturity of affect-related circuitry is associated with better clinical outcomes in young women with sexual trauma, we cannot determine the temporal order or causal relation between brain maturity and outcomes. For example, disrupted neurodevelopment could be an outcome rather than an underlying mechanism of trauma-related symptoms (e.g., Muetzel et al., 2018). Finally, because cross-sectional and longitudinal research on neurodevelopment can lead to different conclusions about the effects of early adversity on brain maturation (e.g., Rakesh & Whittle, 2021), it is important to replicate our results in larger, longitudinal samples.

Another promising direction will be to investigate interactions among trauma characteristics, such as trauma type, chronicity, and timing, on brain development and mental health outcomes. For example, future research with larger samples would be necessary to determine the effects of trauma timing (e.g., age of onset, duration, recency) on the relationship between frontolimbic maturation and mental health outcomes. Due to our limited sample size, we were unable to probe such interactions or control for other trauma characteristics to isolate the unique contributions of trauma type. Despite this limitation, our results underscore the importance of considering trauma characteristics as potential moderators of the relations between trauma exposure and its sequelae. In addition,

because our sample included high-functioning young women on the lower end of the psychopathology spectrum, our results might have been influenced by high levels of resilience in our sample. We suggest that in a clinical sample of sexual trauma survivors with more severe symptoms and higher diagnostic rates, we would observe less affective network maturity compared to nonsexual trauma survivors.

Conclusion

Our results suggest that exposure to sexual trauma during formative years of brain development is associated with greater functional maturity of affect-related brain circuitry in emerging adulthood. Accelerated functional maturation of affective circuitry might represent an adaptation that protects survivors of early sexual trauma from adverse clinical outcomes later in life. In contrast, failure to accelerate maturation of affect-related circuitry following early sexual trauma might confer vulnerability to mental health problems in adulthood. Given the prolonged developmental trajectory of affect-related circuitry, functional maturity of affect-related circuits might hold prognostic or diagnostic promise as a potential neural marker of resilience or vulnerability to negative clinical outcomes in emerging adulthood. For example, interventions that improve clinical outcomes in young survivors of early-life sexual trauma might normalize the maturational trajectory or promote compensatory developmental processes, such as accelerated maturation, in affect-related circuits. Establishing the clinical utility of affective network maturity as a potential resilience or vulnerability marker is a promising avenue for future work.

Competing interests. None.

References

Albaugh, M. D., Ducharme, S., Karama, S., Watts, R., Lewis, J. D., Orr, C., Nguyen, T.-V., Mckinstry, R. C., Botteron, K. N., Evans, A. C., & Hudziak, J. J. (2017). Anxious/depressed symptoms are related to microstructural maturation of white matter in typically developing youths. *Development and Psychopathology*, *29*(3), 751–758. https://doi.org/10.1017/S0954579416000444

Andersen, S. L., & Teicher, M. H. (2008). Stress, sensitive periods and maturational events in adolescent depression. *Trends in Neurosciences*, *31*(4), 183–191. https://doi.org/10.1016/j.tins.2008.01.004

Barch, D. M., Donohue, M. R., Elsayed, N. M., Gilbert, K., Harms, M. P., Hennefield, L., Herzberg, M., Kandala, S., Karcher, N. R., Jackson, J. J., Luking, K. R., Rappaport, B. I., Sanders, A., Taylor, R., Tillman, R., Vogel, A. C., Whalen, D., & Luby, J. L. (2022). Early childhood socioeconomic status and cognitive and adaptive outcomes at the transition to adulthood: The mediating role of gray matter development across five scan waves. *Biological Psychiatry: Cognitive Neuroscience and Neuroimaging*, *7*(1), 34–44. https://doi.org/10.1016/j.bpsc.2021.07.002

Bath, K. G., Manzano-Nieves, G., & Goodwill, H. (2016). Early life stress accelerates behavioral and neural maturation of the hippocampus in male mice. *Hormones and Behavior*, *82*, 64–71. https://doi.org/10.1016/j.yhbeh.2016.04.010

Beck, A., Steer, R., & Brown, G. (1996). *Manual for Beck Depression Inventory II (BDI-II)*. Psychology Corporation. https://doi.org/10.1037/t00742-000

Belsky, J., & Shalev, I. (2016). Contextual adversity, telomere erosion, pubertal development, and health: Two models of accelerated aging, or one? *Development and Psychopathology*, *28*(4), 1367–1383. https://doi.org/10.1017/s0954579416000900

Bick, J., & Nelson, C. A. (2016). Early adverse experiences and the developing brain. *Neuropsychopharmacology*, *41*(1), 177–196. https://doi.org/10.1038/npp.2015.252

Bloom, P. A., VanTieghem, M., Gabard-Durnam, L., Gee, D. G., Flannery, J., Caldera, C., Goff, B., Telzer, E. H., Humphreys, K. L., Fareri, D. S., Shapiro, M., Algharazi, S., Bolger, N., Aly, M., & Tottenham, N. (2022). Age-related change in task-evoked amygdala—prefrontal circuitry: A multiverse approach with an accelerated longitudinal cohort aged 4-22 years. *Human Brain Mapping*, *43*(10), 3221–3244. https://doi.org/10.1002/hbm.25847

Brieant, A. E., Sisk, L. M., & Gee, D. G. (2021). Associations among negative life events, changes in cortico-limbic connectivity, and psychopathology in the ABCD Study. *Developmental Cognitive Neuroscience*, *52*, 101022. https://doi.org/10.1016/j.dcn.2021.101022

Busso, D. S., McLaughlin, K. A., Brueck, S., Peverill, M., Gold, A. L., & Sheridan, M. A. (2017). Child abuse, neural structure, and adolescent psychopathology: A longitudinal study. *Journal of the American Academy of Child & Adolescent Psychiatry*, *56*(4), 321–328. https://doi.org/10.1016/j.jaac.2017.01.013

Callaghan, B. L., Sullivan, R. M., Howell, B., & Tottenham, N. (2014). The international society for developmental psychobiology Sackler symposium: Early adversity and the maturation of emotion circuits—A cross-species analysis. *Developmental Psychobiology*, *56*(8), 1635–1650. https://doi.org/10.1002/dev.21260

Callaghan, B. L., & Tottenham, N. (2016). The stress acceleration hypothesis: Effects of early-life adversity on emotion circuits and behavior. *Current Opinion in Behavioral Sciences*, *7*, 76–81. https://doi.org/10.1016/j.cobeha.2015.11.018

Cohen, S., Kamarck, T., & Mermelstein, R. (1983). A global measure of perceived stress. *Journal of Health and Social Behavior*, *24*(4), 385–396. https://doi.org/10.2307/2136404

Cohodes, E. M., Kitt, E. R., Baskin-Sommers, A., & Gee, D. G. (2020). Influences of early-life stress on frontolimbic circuitry: Harnessing a dimensional approach to elucidate the effects of heterogeneity in stress exposure. *Developmental Psychobiology*, *63*(2), 153–172. https://doi.org/10.1002/dev.21969

Colich, N. L., Platt, J. M., Keyes, K. M., Sumner, J. A., Allen, N. B., & McLaughlin, K. A. (2019). Earlier age at menarche as a transdiagnostic mechanism linking childhood trauma with multiple forms of psychopathology in adolescent girls. *Psychological Medicine*, *50*(7), 1090–1098. https://doi.org/10.1017/s0033291719000953

Colich, N. L., Rosen, M. L., Williams, E. S., & McLaughlin, K. A. (2020). Biological aging in childhood and adolescence following experiences of threat and deprivation: A systematic review and meta-analysis. *Psychological Bulletin*, *146*(9), 721–764. https://doi.org/10.1037/bul0000270

de Nooij, L., Harris, M. A., Hawkins, E. L., Shen, X., Clarke, T. K., Chan, S. W., Ziermans, T. B., McIntosh, A. M., & Whalley, H. C. (2020). Longitudinal trajectories of brain age in young individuals at familial risk of mood disorder from the Scottish Bipolar Family Study [version 3; peer review: 3 approved]. *Wellcome Open Research*, *4*, 206. https://doi.org/10.12688/wellcomeopenres.15617.3

Dickie, E. W., Anticevic, A., Smith, D. E., Coalson, T. S., Manogaran, M., Calarco, N., Viviano, J. D., Glasser, M. F., Van Essen, D. C., & Voineskos, A. N. (2019). Ciftify: A framework for surface-based analysis of legacy MR acquisitions. *NeuroImage*, *197*, 818–826. https://doi.org/10.1016/j.neuroimage.2019.04.078

Dosenbach, N. U., Nardos, B., Cohen, A. L., Fair, D. A., Power, J. D., Church, J. A., Nelson, S. M., Wig, G. S., Vogel, A. C., Lessov-Schlaggar, C. N., Barnes, K. A., Dubis, J. W., Feczko, E., Coalson, R. S., Pruett, J. R. Jr., Barch, D. M., Petersen, S. E., & Schlaggar, B. L. (2010). Prediction of individual brain maturity using fMRI. *Science*, *329*(5997), 1358–1361. https://doi.org/10.1126/science.1194144

Drobinin, V., Van Gestel, H., Helmick, C. A., Schmidt, M. H., Bowen, C. V., & Uher, R. (2022). The developmental brain age is associated with adversity, depression, and functional outcomes among adolescents. *Biological Psychiatry: Cognitive Neuroscience and Neuroimaging*, *7*(4), 406–414. https://doi.org/10.1016/j.bpsc.2021.09.004

Ducharme, S., Albaugh, M. D., Hudziak, J. J., Botteron, K. N., Nguyen, T. V., Truong, C., Evans, A. C., Karama, S., Ball, W. S., Byars, A. W., Schapiro, M., Bommer, W., Carr, A., German, A., Dunn, S., Rivkin, M. J., Waber, D., Mulkern, R., Vajapeyam, S., . . . O'Neill, J. (2014). Anxious/depressed symptoms are linked to right ventromedial prefrontal cortical thickness maturation in healthy children and young adults. *Cerebral Cortex*, *24*(11), 2941–2950.

Dworkin, E. R., Menon, S. V., Bystrynski, J., & Allen, N. E. (2017). Sexual assault victimization and psychopathology: A review and meta-analysis. *Clinical Psychology Review*, *56*, 65–81. https://doi.org/10.1016/j.cpr.2017.06.002

Esteban, O., Markiewicz, C. J., Blair, R. W., Moodie, C. A., Isik, A. I., Erramuzpe, A., Kent, J. D., Goncalves, M., DuPre, E., Snyder, M., Oya, H., Ghosh, S. S., Wright, J., Durnez, J., Poldrack, R. A., & Gorgolewski, K. J. (2019). fMRIPrep: A robust preprocessing pipeline for functional MRI. *Nature Methods*, *16*(1), 111–116. https://doi.org/10.1038/s41592-018-0235-4

Finkelhor, D., & Browne, A. (1985). The traumatic impact of child sexual abuse: A conceptualization. *American Journal of Orthopsychiatry*, *55*(4), 530–541. https://doi.org/10.1111/j.1939-0025.1985.tb02703.x

First, M., Spitzer, B., R., L., Gibbon, M., & Williams, J. B. W. (2002b). *Structured clinical interview for DSM-IV-TR axis I disorders, research version, non-patient edition (SCID-I/NP, 1/2010 revision)*. Biometrics Research, New York State Psychiatric Institute.

First, M. B., Spitzer, R. L., Gibbon, M., & Williams, J. B. W. (2002a). *Structured clinical interview for DSM-IV axis I disorders, clinician version (SCID-CV)*. Biometrics Research, New York State Psychiatric Institute.

Franke, K., Bublak, P., Hoyer, D., Billiet, T., Gaser, C., Witte, O. W., & Schwab, M. (2020). In vivo biomarkers of structural and functional brain development and aging in humans. *Neuroscience & Biobehavioral Reviews*, *117*, 142–164.

Gabard-Durnam, L. J., Flannery, J., Goff, B., Gee, D. G., Humphreys, K. L., Telzer, E., Hare, T., & Tottenham, N. (2014). The development of human amygdala functional connectivity at rest from 4 to 23 years: A cross-sectional study. *NeuroImage*, *95*, 193–207. https://doi.org/10.1016/j.neuroimage.2014.03.038

Gee, D. G., & Casey, B. J. (2015). The impact of developmental timing for stress and recovery. *Neurobiology of Stress*, 1, 184–194. https://doi.org/10.1016/j.ynstr.2015.02.001

Gee, D. G., Gabard-Durnam, L. J., Flannery, J., Goff, B., Humphreys, K. L., Telzer, E. H., Hare, T. A., Bookheimer, S. Y., & Tottenham, N. (2013). Early developmental emergence of human amygdala-prefrontal connectivity after maternal deprivation. *Proceedings of the National Academy of Sciences*, 110(39), 15638–15643. https://doi.org/10.1073/pnas.1307893110

Gray, M. J., Litz, B. T., Hsu, J. L., & Lombardo, T. W. (2004). Psychometric properties of the life events checklist. *Assessment*, 11(4), 330–341. https://doi.org/10.1177/1073191104269954

Green, J. G., McLaughlin, K. A., Berglund, P. A., Gruber, M. J., Sampson, N. A., Zaslavsky, A. M., & Kessler, R. C. (2010). Childhood adversities and adult psychiatric disorders in the national comorbidity survey replication I: Associations with first onset of DSM-IV disorders. *Archives of General Psychiatry*, 67(2), 113–123. https://doi.org/10.1001/archgenpsychiatry.2009.186

Grydeland, H., Walhovd, K. B., Tamnes, C. K., Westlye, L. T., & Fjell, A. M. (2013). Intracortical myelin links with performance variability across the human lifespan: Results from T1-and T2-weighted MRI myelin mapping and diffusion tensor imaging. *Journal of Neuroscience*, 33(47), 18618–18630. https://doi.org/10.1523/JNEUROSCI.2811-13.2013

Gur, R. E., Moore, T. M., Rosen, A. F. G., Barzilay, R., Roalf, D. R., Calkins, M. E., Ruparel, K., Scott, J. C., Almasy, L., Satterthwaite, T. D., Shinohara, R. T., & Gur, R. C. (2019). Burden of environmental adversity associated with psychopathology, maturation, and brain behavior parameters in youths. *JAMA Psychiatry*, 76(9), 966–975. https://doi.org/10.1001/jamapsychiatry.2019.0943

Hanson, J. L., Hariri, A. R., & Williamson, D. E. (2015). Blunted ventral striatum development in adolescence reflects emotional neglect and predicts depressive symptoms. *Biological Psychiatry*, 78(9), 598–605. https://doi.org/10.1016/j.biopsych.2015.05.010

Herzberg, M. P., McKenzie, K. J., Hodel, A. S., Hunt, R. H., Mueller, B. A., Gunnar, M. R., & Thomas, K. M. (2021). Accelerated maturation in functional connectivity following early life stress: Circuit specific or broadly distributed? *Developmental Cognitive Neuroscience*, 48, 100922. https://doi.org/10.1016/j.dcn.2021.100922

Hoppen, T. H., & Chalder, T. (2018). Childhood adversity as a transdiagnostic risk factor for affective disorders in adulthood: A systematic review focusing on biopsychosocial moderating and mediating variables. *Clinical Psychology Review*, 65, 81–151. https://doi.org/10.1016/j.cpr.2018.08.002

Ji, J. L., Spronk, M., Kulkarni, K., Repovš, G., Anticevic, A., & Cole, M. W. (2019). Mapping the human brain's cortical-subcortical functional network organization. *NeuroImage*, 185, 35–57. https://doi.org/10.1016/j.neuroimage.2018.10.006

Joëls, M., & Baram, T. Z. (2009). The neuro-symphony of stress. *Nature Reviews Neuroscience*, 10(6), 459–466. https://doi.org/10.1038/nrn2632

Kaufman, J., Birmaher, B., Brent, D., Rao, U. M. A., Flynn, C., Moreci, P., Williamson, D., & Ryan, N. (1997). Schedule for affective disorders and schizophrenia for school-age children-present and lifetime version (K-SADS-PL): Initial reliability and validity data. *Journal of the American Academy of Child & Adolescent Psychiatry*, 36(7), 980–988. https://doi.org/10.1097/00004583-199707000-00021

Keding, T. J., Heyn, S. A., Russell, J. D., Zhu, X., Cisler, J., McLaughlin, K. A., & Herringa, R. J. (2021). Differential patterns of delayed emotion circuit maturation in abused girls with and without internalizing psychopathology. *American Journal of Psychiatry*, 178(11), 1026–1036. https://doi.org/10.1176/appi.ajp.2021.20081192

Kelly, P. A., Viding, E., Wallace, G. L., Schaer, M., De Brito, S. A., Robustelli, B., & McCrory, E. J. (2013). Cortical thickness, surface area, and gyrification abnormalities in children exposed to maltreatment: Neural markers of vulnerability? *Biological Psychiatry*, 74(11), 845–852. https://doi.org/10.1016/j.biopsych.2013.06.020

Kessler, R. C., Green, J. G., Adler, L. A., Barkley, R. A., Chatterji, S., Faraone, S. V., Finkelman, M., Greenhill, L. L., Gruber, M. J., Jewell, M., Russo, L. J., Sampson, N. A., & Van Brunt, D. L. (2010). Structure and diagnosis of adult attention-deficit/hyperactivity disorder: Analysis of expanded symptom criteria from the Adult ADHD Clinical Diagnostic Scale. *Archives of General Psychiatry*, 67(11), 1168–1178. https://doi.org/10.1001/archgenpsychiatry.2010.146

Lebel, C., Gee, M., Camicioli, R., Wieler, M., Martin, W., & Beaulieu, C. (2012). Diffusion tensor imaging of white matter tract evolution over the lifespan. *NeuroImage*, 60(1), 340–352. https://doi.org/10.1016/j.neuroimage.2011.11.094

Liang, H., Zhang, F., & Niu, X. (2019). Investigating systematic bias in brain age estimation with application to post-traumatic stress disorders. *Human Brain Mapping*, 40(11), 3143–3152.

Liem, F., Varoquaux, G., Kynast, J., Beyer, F., Kharabian Masouleh, S. K., Huntenburg, J. M., Lampe, L., Rahim, M., Abraham, A., Craddock, R. C., Riedel-Heller, S., Luck, T., Loeffler, M., Schroeter, M. L., Witte, A. V., Villringer, A., & Margulies, D. S. (2017). Predicting brain-age from multimodal imaging data captures cognitive impairment. *Neuroimage*, 148, 179–188.

Manzano Nieves, G., Bravo, M., Baskoylu, S., & Bath, K. G. (2020). Early life adversity decreases pre-adolescent fear expression by accelerating amygdala PV cell development. *Elife*, 9, e55263. https://doi.org/10.7554/eLife.55263

Mendle, J., Leve, L. D., Van Ryzin, M., & Natsuaki, M. N. (2014). Linking childhood maltreatment with girls' internalizing symptoms: Early puberty as a tipping point. *Journal of Research on Adolescence*, 24(4), 689–702. https://doi.org/10.1111/jora.12075

Mendle, J., Ryan, R. M., & McKone, K. M. (2016). Early childhood maltreatment and pubertal development: Replication in a population-based sample. *Journal of Research on Adolescence*, 26(3), 595–602. https://doi.org/10.1111/jora.12201

Molnar, B. E., Buka, S. L., & Kessler, R. C. (2001). Child sexual abuse and subsequent psychopathology: Results from the National Comorbidity Survey. *American Journal of Public Health*, 91(5), 753–760. https://doi.org/10.2105/ajph.91.5.753

Muetzel, R. L., Blanken, L. M., van der Ende, J., El Marroun, H., Shaw, P., Sudre, G., van der Lugt, A., Jaddoe, V. W. V., Verhulst, F. C., Tiemeier, H., & White, T. (2018). Tracking brain development and dimensional psychiatric symptoms in children: A longitudinal population-based neuroimaging study. *American Journal of Psychiatry*, 175(1), 54–62. https://doi.org/10.1176/appi.ajp.2017.16070813

Narvacan, K., Treit, S., Camicioli, R., Martin, W., & Beaulieu, C. (2017). Evolution of deep gray matter volume across the human lifespan. *Human Brain Mapping*, 38(8), 3771–3790. https://doi.org/10.1002/hbm.23604

Neeb, H., Zilles, K., & Shah, N. J. (2006). Fully-automated detection of cerebral water content changes: Study of age-and gender-related H2O patterns with quantitative MRI. *NeuroImage*, 29(3), 910–922. https://doi.org/10.1016/j.neuroimage.2005.08.062

Nielsen, A. N., Greene, D. J., Gratton, C., Dosenbach, N. U., Petersen, S. E., & Schlaggar, B. L. (2019). Evaluating the prediction of brain maturity from functional connectivity after motion artifact denoising. *Cerebral Cortex*, 29(6), 2455–2469. https://doi.org/10.1093/cercor/bhy117

Noll, J. G., Trickett, P. K., Long, J. D., Negriff, S., Susman, E. J., Shalev, I., Li, J. C., & Putnam, F. W. (2017). Childhood sexual abuse and early timing of puberty. *Journal of Adolescent Health*, 60(1), 65–71. https://doi.org/10.1016/j.jadohealth.2016.09.008

Nooner, K. B., Colcombe, S. J., Tobe, R. H., Mennes, M., Benedict, M. M., Moreno, A. L., Panek, L. J., Brown, S., Zavitz, S. T., Li, Q., Sikka, S., Gutman, D., Bangaru, S., Schlachter, R. T., Kamiel, S. M., Anwar, A. R., Hinz, C. M., Kaplan, M. S., Rachlin, A. B., ... Milham, M. P. (2012). The NKI-Rockland sample: A model for accelerating the pace of discovery science in psychiatry. *Frontiers in Neuroscience*, 6, 152. https://doi.org/10.3389/fnins.2012.00152

O'Brien, J. E., White, K., Wu, Q., & Killian-Farrell, C. (2016). Mental health and behavioral outcomes of sexual and nonsexual child maltreatment among child welfare-involved youth. *Journal of Child Sexual Abuse*, 25(5), 483–503. https://doi.org/10.1080/10538712.2016.1167801

Ono, M., Kikusui, T., Sasaki, N., Ichikawa, M., Mori, Y., & Murakami-Murofushi, K. (2008). Early weaning induces anxiety and precocious myelination in the anterior part of the basolateral amygdala of male Balb/c mice. *Neuroscience*, 156(4), 1103–1110. https://doi.org/10.1016/j.neuroscience.2008.07.078

Petanjek, Z., Judaš, M., Šimić, G., Rašin, M. R., Uylings, H. B., Rakic, P., & Kostović, I. (2011). Extraordinary neoteny of synaptic spines in the human

prefrontal cortex. *Proceedings of the National Academy of Sciences*, *108*(32), 13281–13286. https://doi.org/10.1073/pnas.1105108108

Platt, J. M., Colich, N. L., McLaughlin, K. A., Gary, D., & Keyes, K. M. (2017). Transdiagnostic psychiatric disorder risk associated with early age of menarche: A latent modeling approach. *Comprehensive Psychiatry*, *79*, 70–79. https://doi.org/10.1016/j.comppsych.2017.06.010

Pynoos, R., Rodriguez, N., Steinberg, A., Stuber, M., & Frederick, C. (1998). *The University of California at Los Angeles Posttraumatic Stress Disorder Reaction Index (UCLA-PTSD RI)*. UCLA Trauma Psychiatry Program.

Rakesh, D., Cropley, V., Zalesky, A., Vijayakumar, N., Allen, N. B., & Whittle, S. (2021). Neighborhood disadvantage and longitudinal brain-predicted-age trajectory during adolescence. *Developmental Cognitive Neuroscience*, *51*, 101002. https://doi.org/10.1016/j.dcn.2021.101002

Rakesh, D., & Whittle, S. (2021). Socioeconomic status and the developing brain-A systematic review of neuroimaging findings in youth. *Neuroscience & Biobehavioral Reviews*, *130*, 379–407. https://doi.org/10.1016/j.neubiorev.2021.08.027

Raudales, A. M., Short, N. A., & Schmidt, N. B. (2019). Emotion dysregulation mediates the relationship between trauma type and PTSD symptoms in a diverse trauma-exposed clinical sample. *Personality and Individual Differences*, *139*, 28–33. https://doi.org/10.1016/j.paid.2018.10.033

Smola, A. J., & Schölkopf, B. (2004). A tutorial on support vector regression. *Statistics and Computing*, *14*(3), 199–222. https://doi.org/10.1023/B:STCO.0000035301.49549.88

Spielberger, C. D., Gorsuch, R. L., Lushene, R., Vagg, P. R., & Jacobs, G. A. (1983). *Manual for the state-trait anxiety inventory*. Consulting Psychologists Press.

Sumner, J. A., Colich, N. L., Uddin, M., Armstrong, D., & McLaughlin, K. A. (2019). Early experiences of threat, but not deprivation, are associated with accelerated biological aging in children and adolescents. *Biological Psychiatry*, *85*(3), 268–278. https://doi.org/10.1016/j.biopsych.2018.09.008

Thijssen, S., Collins, P. F., & Luciana, M. (2022). Does pubertal stage mediate the association between family environment and structure and function of the amygdala-mPFC circuit? A replication study of the longitudinal ABCD cohort. *Developmental Cognitive Neuroscience*, *56*, 101120.

Tian, L., Ma, L., & Wang, L. (2016). Alterations of functional connectivities from early to middle adulthood: Clues from multivariate pattern analysis of resting-state fMRI data. *NeuroImage*, *129*, 389–400.

Tyborowska, A., Volman, I., Niermann, H. C., Pouwels, J. L., Smeekens, S., Cillessen, A. H., Toni, I., & Roelofs, K. (2018). Early-life and pubertal stress differentially modulate grey matter development in human adolescents. *Scientific Reports*, *8*(1), 1–11. https://doi.org/10.1038/s41598-018-27439-5

Vanes, L. D., Moutoussis, M., Ziegler, G., Goodyer, I. M., Fonagy, P., Jones, P. B., Bullmore, E. T., & Dolan, R. J. (2020). White matter tract myelin maturation and its association with general psychopathology in adolescence and early adulthood. *Human Brain Mapping*, *41*(3), 827–839. https://doi.org/10.1002/hbm.24842

VanTieghem, M. R., & Tottenham, N. (2017). Neurobiological programming of early life stress: Functional development of amygdala-prefrontal circuitry and vulnerability for stress-related psychopathology. In E. Vermetten, D. Baker, & V. Risbrough (Eds.), *Behavioral neurobiology of PTSD* (pp. 117–136). Springer. https://doi.org/10.1007/7854_2016_42

Vapnik, V. N. (1995). *The nature of statistical learning theory*. Springer.

Watson, D., Clark, L. A., & Tellegen, A. (1988). Development and validation of brief measures of positive and negative affect: The PANAS scales. *Journal of Personality and Social Psychology*, *54*(6), 1063–1070.

Weathers, F. W., Bovin, M. J., Lee, D. J., Sloan, D. M., Schnurr, P. P., Kaloupek, D. G., Keane, T. M., & Marx, B. P. (2018). The Clinician-Administered PTSD Scale for DSM-5 (CAPS-5): Development and initial psychometric evaluation in military veterans. *Psychological Assessment*, *30*(3), 383–395. https://doi.org/10.1037/pas0000486

Whittle, S., Dennison, M., Vijayakumar, N., Simmons, J. G., Yücel, M., Lubman, D. I., Pantelis, C., & Allen, N. B. (2013). Childhood maltreatment and psychopathology affect brain development during adolescence. *Journal of the American Academy of Child & Adolescent Psychiatry*, *52*(9), 940–952. https://doi.org/10.1016/j.jaac.2013.06.007

Whittle, S., Vijayakumar, N., Dennison, M., Schwartz, O., Simmons, J. G., Sheeber, L., Allen, N. B., & Rosenfeld, C. S. (2016). Observed measures of negative parenting predict brain development during adolescence. *PloS One*, *11*(1), e0147774. https://doi.org/10.1371/journal.pone.0147774

Supplementary Information

1.1 Neuroimaging data preprocessing

An overview of the neuroimaging data preprocessing pipeline is presented in Figure S1. Anatomical T1w scans and resting-state functional scans were preprocessed using the fMRIPrep workflow (1.4.1rc1; https://fmriprep.readthedocs.io/en/stable/; Esteban et al., 2019; RRID:SCR_016216) based on Nipype 1.2.0 (Gorgolewski et al., 2011; RRID:SCR_002502), which combines tools from multiple software packages. Many internal operations of fMRIPrep use Nilearn (RRID:SCR_001362), principally within the functional data preprocessing workflow.

Structural data preprocessing. Each structural image was visually inspected, and images affected by severe motion artifacts were excluded. T1w images were corrected for intensity nonuniformity (INU) with N4BiasFieldCorrection v2.1.0 (Tustison et al., 2010), distributed with ANTs 2.2.0 (Avants et al., 2008; RRID:SCR_004757). The INU-corrected T1w image was used as a T1w-reference image throughout the workflow. When several T1w images were available for the same participant, a T1w-reference image was computed by co-registering and averaging the INU-corrected T1w images using mri_robust_template (FreeSurfer 6.0.1, Dale et al., 1999). When three or more T1w images were available, an unbiased T1w template equidistant from all T1w images was generated. The T1w-reference image was then skull-stripped with a Nipype implementation of the antsBrainExtraction.sh v2.1.0 workflow (ANTs), using OASIS30ANTs as target template.

The skull-stripped T1w reference image was then segmented into cerebrospinal fluid (CSF), white matter (WM), and gray matter (GM) using FAST (FSL 5.0.9, RRID:SCR_002823, Zhang et al., 2001). Brain surfaces were reconstructed using recon-all (FreeSurfer 6.0.1, RRID:SCR_001847, Dale et al., 1999). The brain mask initially generated using ANTs was refined with a custom variation of a method that reconciles ANTs-derived and FreeSurfer-derived segmentations of the cortical gray matter (RRID:SCR_002438, Klein et al., 2017). The T1w reference image was co-registered to a standard template in MNI space (ICBM 152 nonlinear asymmetrical template version 2009c, MNI152NLin2009cAsym; Fonov et al., 2009; RRID:SCR_008796) using nonlinear registration with antsRegistration (ANTs 2.2.0), using brain-extracted versions of both T1w reference and the standard template.

Functional data preprocessing. For each resting-state functional run, the following preprocessing was performed. First, a reference functional volume and its skull-stripped version were generated using a custom methodology of fMRIPrep. When non-steady-state volumes were detected, they were averaged and used as a reference due to their enhanced tissue contrast. Alternatively, the median of a motion-corrected subset of volumes was used as a functional reference image. Head-motion parameters with respect to the functional reference image (i.e., transformation matrices and six corresponding rotation and translation parameters) were estimated using six-degree-of-freedom registration in MCFLIRT (FSL 5.0.9, Jenkinson et al., 2002).

A deformation field to correct for susceptibility distortions was estimated based on fMRIPrep's fieldmap-less approach based on the ANTs symmetric normalization (SyN) technique. The deformation field is that resulting from co-registering the functional reference to the same-subject T1w-reference with its intensity inverted (Wang et al., 2017; Huntenburg, 2014). Registration was performed with antsRegistration (ANTs 2.2.0), regularized by constraining deformation to be nonzero only along the phase-encoding direction, and modulated with an average fieldmap template (Treiber et al., 2016). Based on the estimated susceptibility distortion, an unwarped functional reference image was calculated for a more accurate co-registration with the anatomical reference image. The functional reference image was then co-registered to the T1w reference image using bbregister (FreeSurfer) which implements boundary-based registration (Greve & Fischl, 2009). Co-registration was configured with nine degrees of freedom to account for distortions remaining in the functional reference.

The functional time-series were resampled onto their native space by applying a single, composite transform to correct for head-motion and susceptibility distortions, to generate a preprocessed functional run in native space. The functional time-series were also resampled into standard volume space (MNI152NLin2009cAsym space) and onto the fsaverage5 standard surface. All resamplings were performed with a single interpolation step by composing all the pertinent transformations (i.e., head-motion parameters, susceptibility distortion correction, and co-registrations to anatomical [EPI-to-T1w] and reference spaces [T1w-to-MNI]). Volumetric resampling was performed using antsApplyTransforms (ANTs v2.1.0), configured with Lanczos interpolation to minimize the smoothing effects of other kernels (Lanczos, 1964). Surface resampling was performed using mri_vol2surf (FreeSurfer), by sampling the cortical ribbon at six intervals and assigning the average to each vertex.

Estimation of confound timeseries. Several confounding timeseries were calculated based on the preprocessed functional data. Framewise displacement (FD) and average change in mean intensity between each pair of fMRI volumes (DVARS) were calculated using their implementations in Nipype, following the definitions by Power et al. (2014). The three global signals were extracted within the CSF, the WM, and the whole-brain masks. The confound time series derived from head motion estimates and global signals were expanded with the inclusion of temporal derivatives and quadratic terms for each (Satterthwaite et al., 2013).

Conversion to CIFTI format. We converted the anatomical and functional data outputs of the fMRIPrep preprocessing pipeline to the Connectivity Informatics Technology Initiative (CIFTI; https://www.nitrc.org/projects/cifti/) format, which is compatible with HCP tools and offers a number of advantages over traditional volume (e.g., NIFTI) and surface (e.g., GIFTI) formats (e.g., Coalson et al., 2018). For example, in CIFTI format, cortical gray matter which conforms best to 2D geometry is stored as surface vertices, whereas subcortical structures which have globular 3D morphology are stored as subcortical voxels (e.g., Glasser et al., 2013). In addition, in CIFTI format, high-resolution neuroimaging data can be condensed into a set of gray matter coordinates (i.e., cortical surface vertices and subcortical voxels collectively known as "grayordinates"), which allows for a more compact representation and smaller file size (e.g., ~200k voxels in a standard 2mm isotropic volume space vs. ~90k grayordinates in the standard CIFTI space).

To convert the preprocessed data to the CIFTI format, we used the fmriprep_ciftify BIDS-app (Dickie et al., 2019; https://github.com/edickie/ciftify). This tool was adapted from the HCP minimal preprocessing pipelines to convert legacy neuroimaging data that do not meet the HCP data acquisition standards to the formats compatible with HCP tools (Glasser et al., 2013). As part of the structural fmriprep_ciftify workflow (ciftify_recon_all): 1) FreeSurfer output surfaces were converted to GIFTI and CIFTI formats, and 2) the native cortical meshes were aligned and resampled to the standard 32k fs_LR mesh using the MSMSulc algorithm, which aligns surfaces based on sulcal anatomy (Robinson et al., 2018). The 32k fs_LR mesh is a bilaterally symmetrical standard surface mesh that consists of vertices spaced about 2 mm apart and is best suited for the low-resolution fMRI data (Glasser et al., 2013). T1w images and volumetric outputs of the FreeSurfer pipeline were nonlinearly co-registered to the MNI standard space using FSL's FNIRT, which unlike the spatial normalization in fMRIPrep (using ANTs), generates less distortion and does not overfit to folding patterns (Dickie et al., 2019).

As part of the functional fmriprep_ciftify workflow (ciftify_subject_fmri), preprocessed functional runs in T1w volume space (NIFTI format) were projected onto each participant's grayordinate space (CIFTI dense timeseries format). Resampling of cortical data was performed using a weighted, ribbon-constrained approach, using the cortical gray matter ribbon generated by FreeSurfer, after excluding excessively noisy voxels. Resampling of subcortical data was performed in a subcortical parcel-constrained manner using subcortical parcels which were generated by FreeSurfer segmentation. Surface (cortical vertices) and volumetric (subcortical voxels) timeseries in native space were mapped onto the standard grayordinate space (~32k

subcortical voxels and ~32k cortical vertices in each hemisphere). All subsequent denoising operations and analyses were performed on the functional data in CIFTI format.

1.2 Denoising of the resting-state functional data

Motion quantification. Head motion has been shown to artificially inflate functional connectivity estimates for short-distance connections and decrease functional connectivity estimates for long-distance connections (e.g., Power et al., 2012). For each functional run, we calculated two quality control measures related to head motion: framewise displacement (FD; Power et al., 2014), an index of head displacement between adjacent timepoints, and DVARS (Smyser et al., 2010), an index of change in global intensity between adjacent timepoints.

Following Burgess et al. (2016), DVARS were calculated on the minimally preprocessed CIFTI dense timeseries after intensity normalization to a global mean of 10,000. DVARS were then median centered to control for differences in thermal noise across participants, which have been linked to differences in head size (Burgess et al., 2016). For each functional run, we quantified contamination by head motion using the following measures: mean FD and number of timepoints contaminated by motion with FD > 0.39 mm and/or DVARS > 4.9 (Burgess et al., 2016). We excluded functional runs with < 4 minutes of data uncontaminated by motion (i.e., FD < 0.39 mm and DVARS < 4.9). This resulted in exclusion of 6 participants from the training dataset, such that the final sample used to train the normative models included 79 participants (M_{age} = 23.2, SD_{age} = 11.8, range: 6-45). No participants were excluded from the test dataset.

Denoising approach. To minimize the effects of head motion and other sources of noise and global artifacts on resting-state functional connectivity, we performed the following steps using custom Matlab code (MATLAB_R2019b). Resting-state functional data in CIFTI format, which had been minimally preprocessed using fMRIPrep, were intensity normalized to a global 4D mean of 10,000. We then built a general linear model with the following regressors: constant, linear, and quadratic terms, 6 head motion parameters and their squares, first-order temporal derivatives of the 6 motion parameters and their squares, mean tissue and global signals and their squares, first-order temporal derivatives of the mean tissue and global signals and their squares (e.g., Parkes et al., 2018). All regressors, with the exception of the constant, linear, and quadratic terms, were normalized prior to inclusion in the model. Variance associated with each of the 39 nuisance regressors was then regressed out of the minimally preprocessed and intensity-normalized resting-state fMRI data. Following nuisance regression, cleaned functional data were temporally filtered using a second-order zero-phase Butterworth filter with a high-pass cut-off frequency of 0.009 Hz (Burgess et al., 2016).
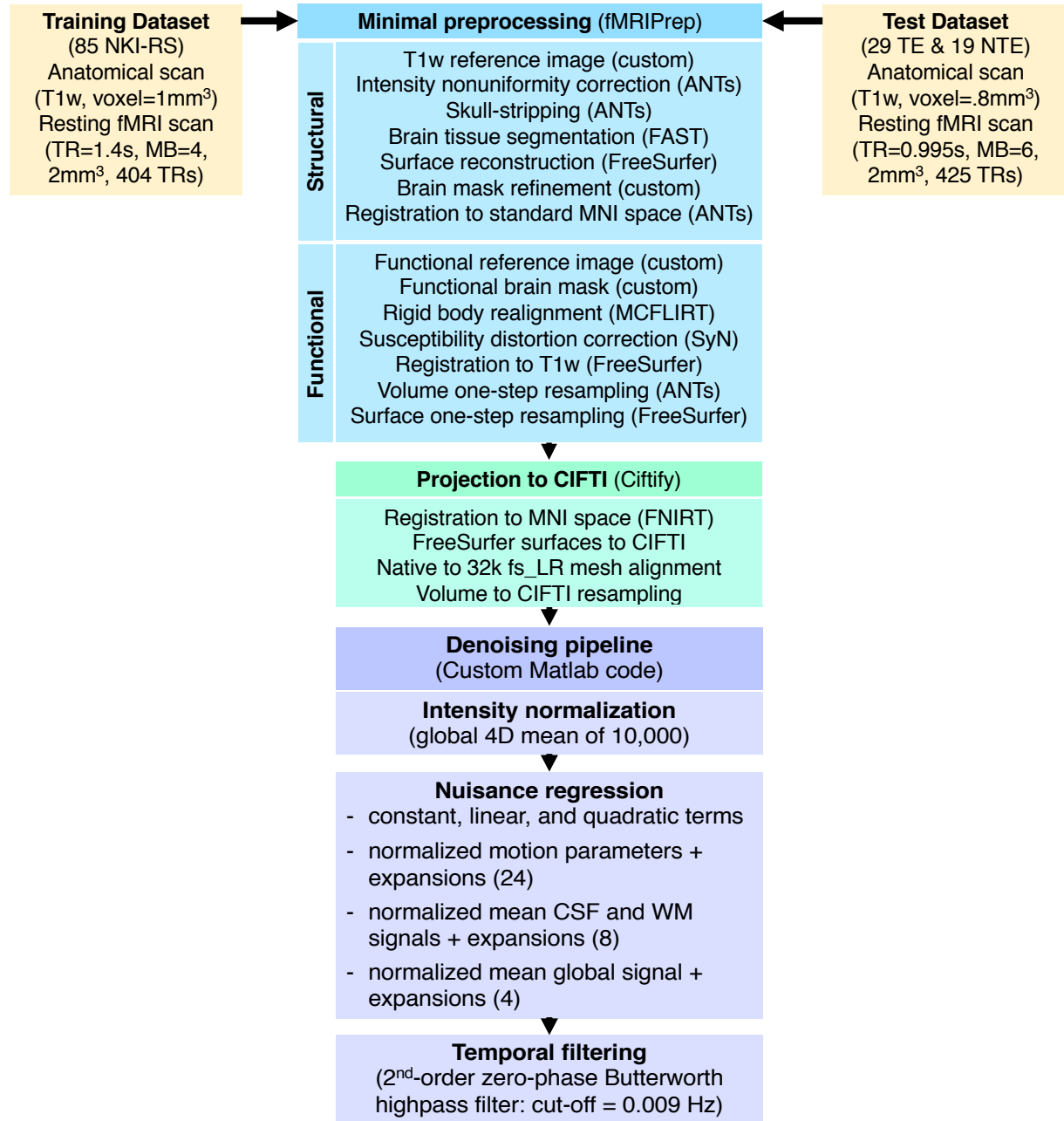
Training Dataset	Minimal preprocessing (fMRIPrep)	Test Dataset

Training Dataset
(85 NKI-RS)
Anatomical scan
(T1w, voxel=1mm³)
Resting fMRI scan
(TR=1.4s, MB=4,
2mm³, 404 TRs)

Minimal preprocessing (fMRIPrep)

Structural
T1w reference image (custom)
Intensity nonuniformity correction (ANTs)
Skull-stripping (ANTs)
Brain tissue segmentation (FAST)
Surface reconstruction (FreeSurfer)
Brain mask refinement (custom)
Registration to standard MNI space (ANTs)

Functional
Functional reference image (custom)
Functional brain mask (custom)
Rigid body realignment (MCFLIRT)
Susceptibility distortion correction (SyN)
Registration to T1w (FreeSurfer)
Volume one-step resampling (ANTs)
Surface one-step resampling (FreeSurfer)

Test Dataset
(29 TE & 19 NTE)
Anatomical scan
(T1w, voxel=.8mm³)
Resting fMRI scan
(TR=0.995s, MB=6,
2mm³, 425 TRs)

Projection to CIFTI (Ciftify)

Registration to MNI space (FNIRT)
FreeSurfer surfaces to CIFTI
Native to 32k fs_LR mesh alignment
Volume to CIFTI resampling

Denoising pipeline
(Custom Matlab code)

Intensity normalization
(global 4D mean of 10,000)

Nuisance regression
- constant, linear, and quadratic terms
- normalized motion parameters + expansions (24)
- normalized mean CSF and WM signals + expansions (8)
- normalized mean global signal + expansions (4)

Temporal filtering
(2nd-order zero-phase Butterworth
highpass filter: cut-off = 0.009 Hz)

Figure S1. Overview of the preprocessing and denoising workflows.

1.3 Functional connectivity estimation

All functional connectivity estimation operations were performed on the cleaned and filtered functional data using custom Matlab code and Connectome Workbench v1.4.2 (https://www.humanconnectome.org/software/workbench-command). An overview of the functional connectivity estimation workflow is presented in Figure S8.

Parcellation scheme. We used the Cole-Anticevic Brain-wide Network Partition (CAB-NP v1.1) to parcellate the brain into 718 regions of interest (ROIs; 360 cortical and 358 subcortical) organized into 12 functional networks: primary visual, secondary visual, somatomotor, cingulo-opercular, dorsal attention, language, frontoparietal, auditory, default mode, posterior

multimodal, ventral multimodal, and orbito-affective (Ji et al., 2019; https://github.com/ColeLab/ColeAnticevicNetPartition; see Figure S2). This network partition was generated using the HCP's multimodal cortical parcellation atlas (HCP_MMP1.0; Glasser et al., 2016), which consists of 180 cortical parcels in each hemisphere. The network partition was further extended into subcortical gray matter by assigning each subcortical voxel to the cortical network with which it had the strongest average correlation (Ji et al., 2019).
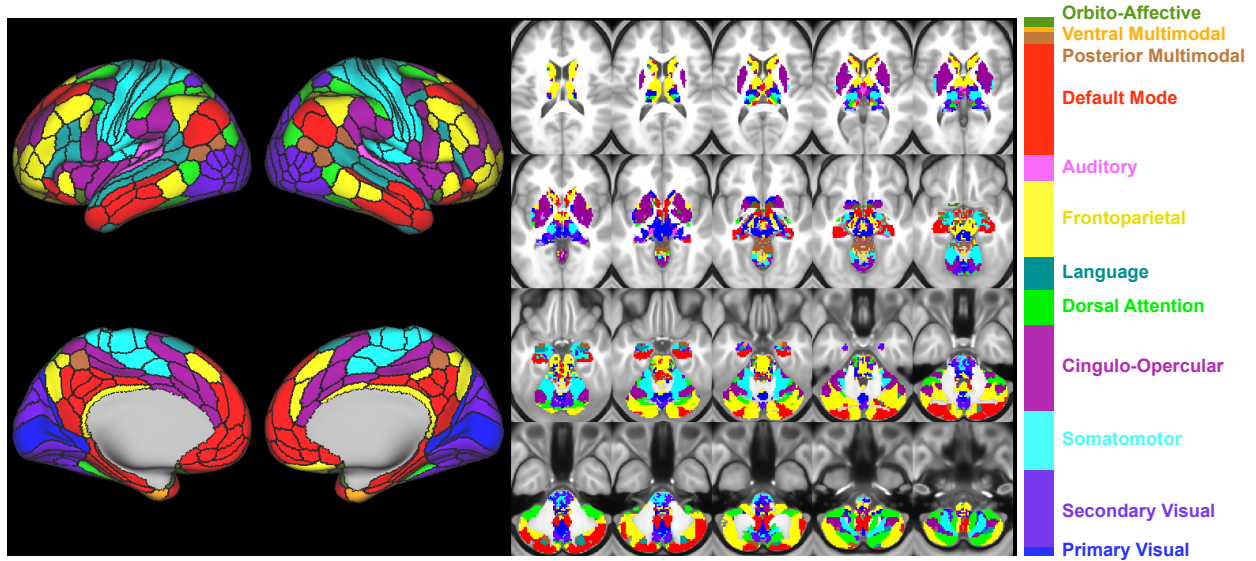
Figure S2. The Cole-Anticevic Brain-wide Network Partition (CAB-NP v1.1) was used to parcellate the brain into 360 cortical and 358 subcortical regions of interest organized into 12 functional networks.

We extracted mean timeseries from each of the 718 ROIs within the CAB-NP atlas using wb_command -cifti-parcellate. Prior to estimating functional connectivity between each pair of ROIs, we discarded the first eight timepoints to allow for magnetic equilibration. As a result, we used a total of 396 volumes for each participant in the training dataset and 417 volumes for each participant in the test dataset. For each participant in the training dataset, we calculated temporal signal-to-noise ratio (tSNR) for each of the 718 ROIs. We then created a group median tSNR map (see Figure S3) and excluded ROIs with median tSNR < 100 (151 ROIs; 21% of total ROIs). All excluded ROIs were subcortical and located either near the borders of the field-of-view or in the areas of EPI signal dropout.
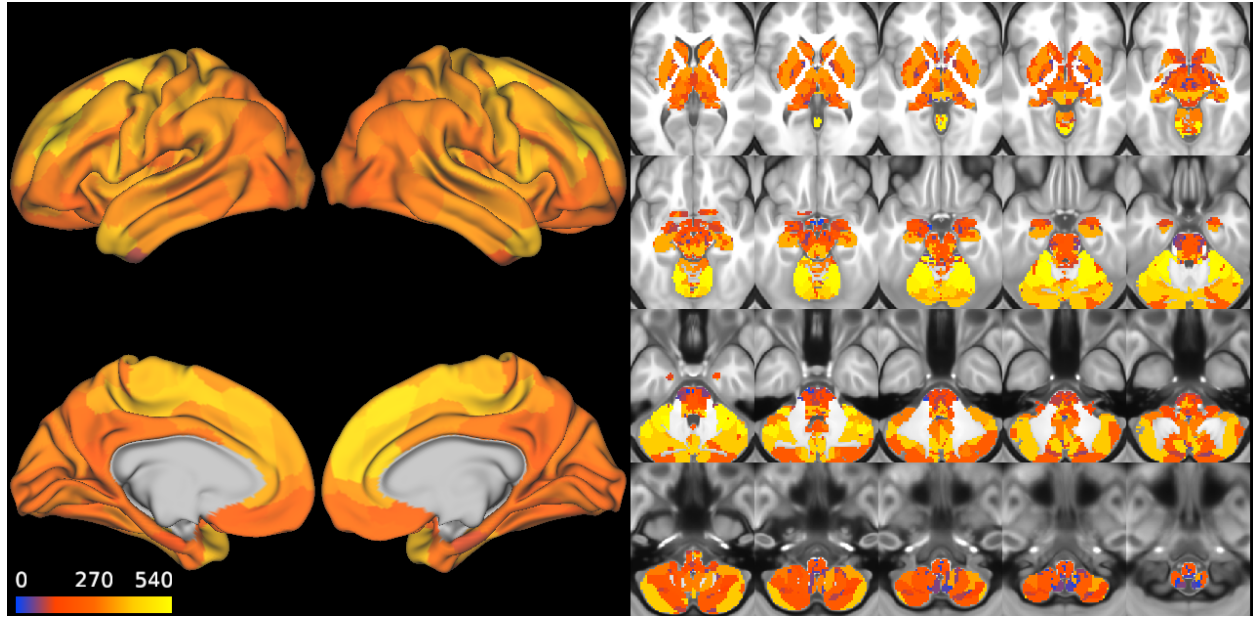
Figure S3. Group median temporal signal-to-noise ratio (tSNR) for each of the 718 ROIs in the Cole-Anticevic Brain-wide Network Partition atlas (CAB-NP v1.1). ROIs with median tSNR < 100 (purple-blue) were excluded from the analyses.

We used the remaining 567 ROIs to compute pairwise functional connectivity by calculating Pearson's correlation coefficients between each pair of ROIs. Correlation coefficients were then converted to Z-scores using Fisher's r-to-Z transformation. As a result, each participant had a 567 x 567 functional connectivity matrix (160,461 unique functional connections or edges) which was then used for estimation of functional brain maturity (see Figure S4).
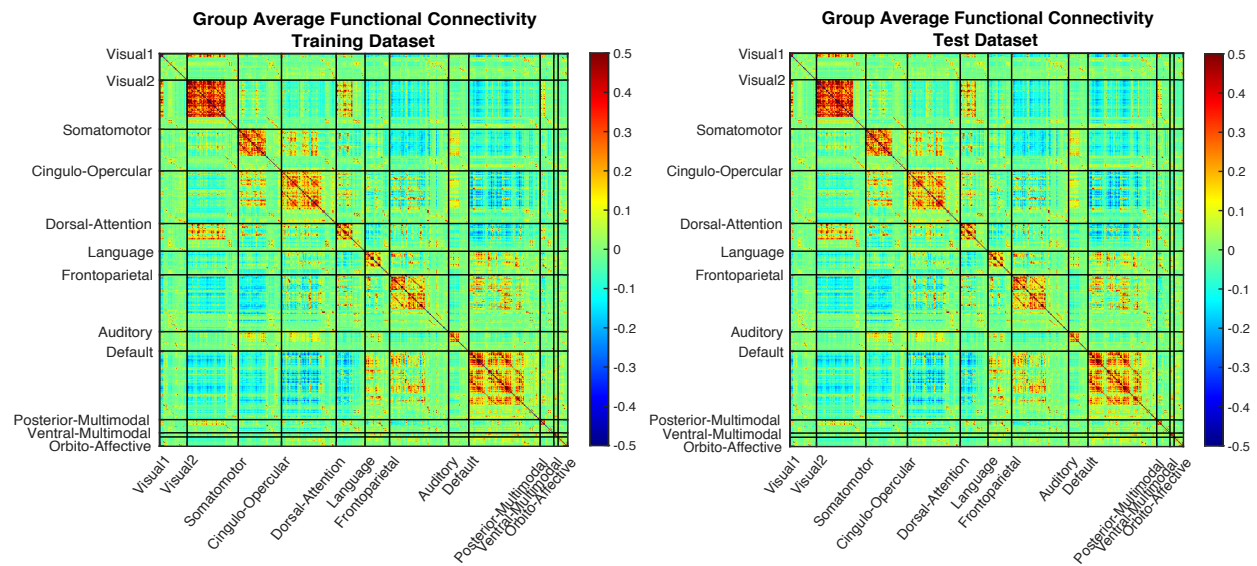
Figure S4. Group mean functional connectivity matrices for the training (left panel) and test (right panel) datasets.

Quality control. To determine whether our denoising approach was successful and estimate the amount of residual motion in the cleaned and filtered functional data, as well as its effects on functional connectivity, we performed the following quality control steps. We plotted the distributions of functional connectivity estimates (Fisher r-to-Z-transformed correlation coefficients) for the training and test datasets (see Figure S5). Consistent with the previously reported effects of global signal regression on functional connectivity (e.g., Ciric et al., 2017), both distributions of functional connectivity estimates were normal in shape and centered on zero.
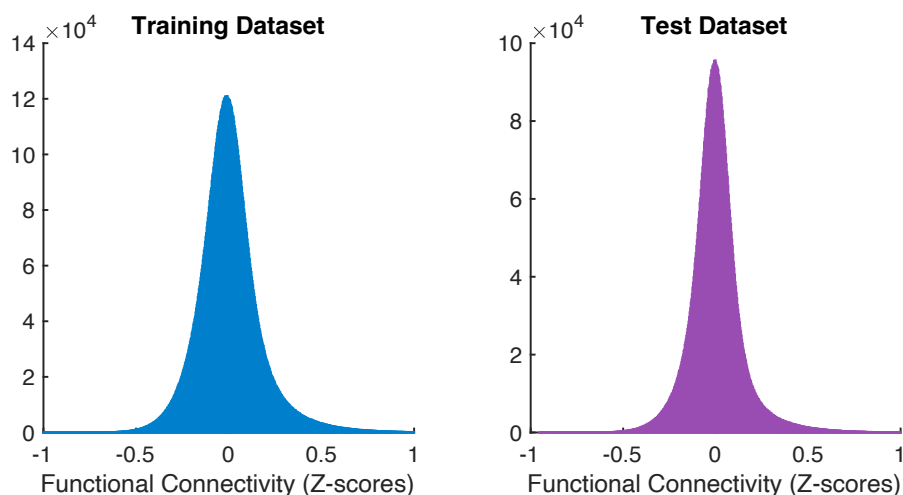

Figure S5. Distributions of functional connectivity estimates (Z-scores) in the training dataset (left panel) and the test dataset (right panel). Consistent with the previously reported effects of global signal regression (e.g., Ciric et al., 2017), both distributions of functional connectivity estimates were normal in shape and centered on zero.

In addition, we calculated correlations between each edge (i.e., functional connection between a given pair of ROIs) and mean FD in the training and test datasets (Figure S6). In the training dataset, 39% of edges were correlated with FD at uncorrected $p < 0.05$ and 28% of edges were correlated with FD at FDR-corrected $p < 0.05$. In the test dataset, 9% of edges were correlated with FD at uncorrected $p < 0.05$ and none were correlated with FD at FDR-corrected $p < 0.05$ (Figure S7). To minimize the effects of residual motion on functional connectivity estimates in the training dataset, we excluded edges that were correlated with FD at uncorrected $p < 0.05$ in the training dataset from all subsequent analyses. The same edges were also excluded from the test dataset.
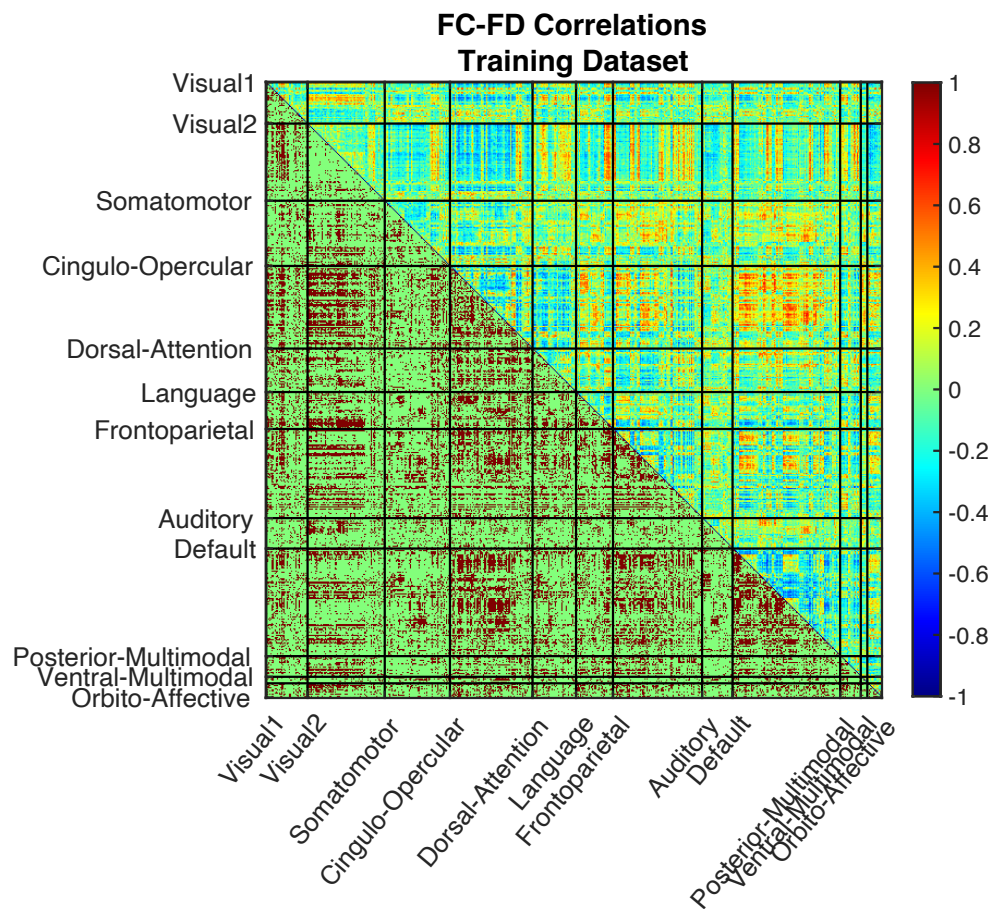
Figure S6. Correlations between functional connectivity (FC) estimates and mean framewise displacement (FD). The upper triangle of the matrix shows correlation coefficients, whereas the lower triangle shows statistical significance of the FC-FD correlations. In the lower triangle, edges that are correlated with FD below the FDR-corrected threshold of p = 0.05 are shown in brown, whereas edges that are not correlated with FD are shown in green. Functional connections correlated with FD below the uncorrected threshold of p = 0.05 were excluded from subsequent analyses.
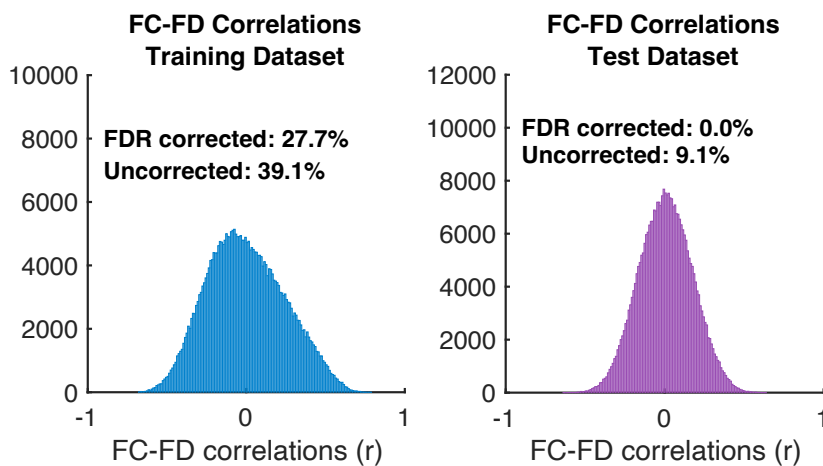
Figure S7. Distributions of correlation coefficients between functional connectivity (FC) estimates and mean framewise displacement (FD) in the training dataset (left panel) and the test dataset (right panel). In the training dataset, 39% of edges were correlated with FD at uncorrected p < 0.05 *and 28% of edges were correlated with FD at FDR-corrected* p < 0.05. *In the test dataset, 9% of edges were correlated with FD at uncorrected* p < 0.05 *and none were correlated with FD at FDR-corrected* p < 0.05.

1.4 Training the normative model of affective network maturation

We used machine learning to train the normative model of affective network maturation using the functional connectivity matrices of the selected NKI-RS participants as the training dataset and the functional connectivity matrices of the trauma-exposed participants as the test dataset. All machine learning operations were performed in Matlab R2019b using the Statistics and Machine Learning Toolbox and the Regression Learner App (Natick, Massachusetts, The MathWorks Inc.). An overview of the machine learning workflow is presented in Figure S8.
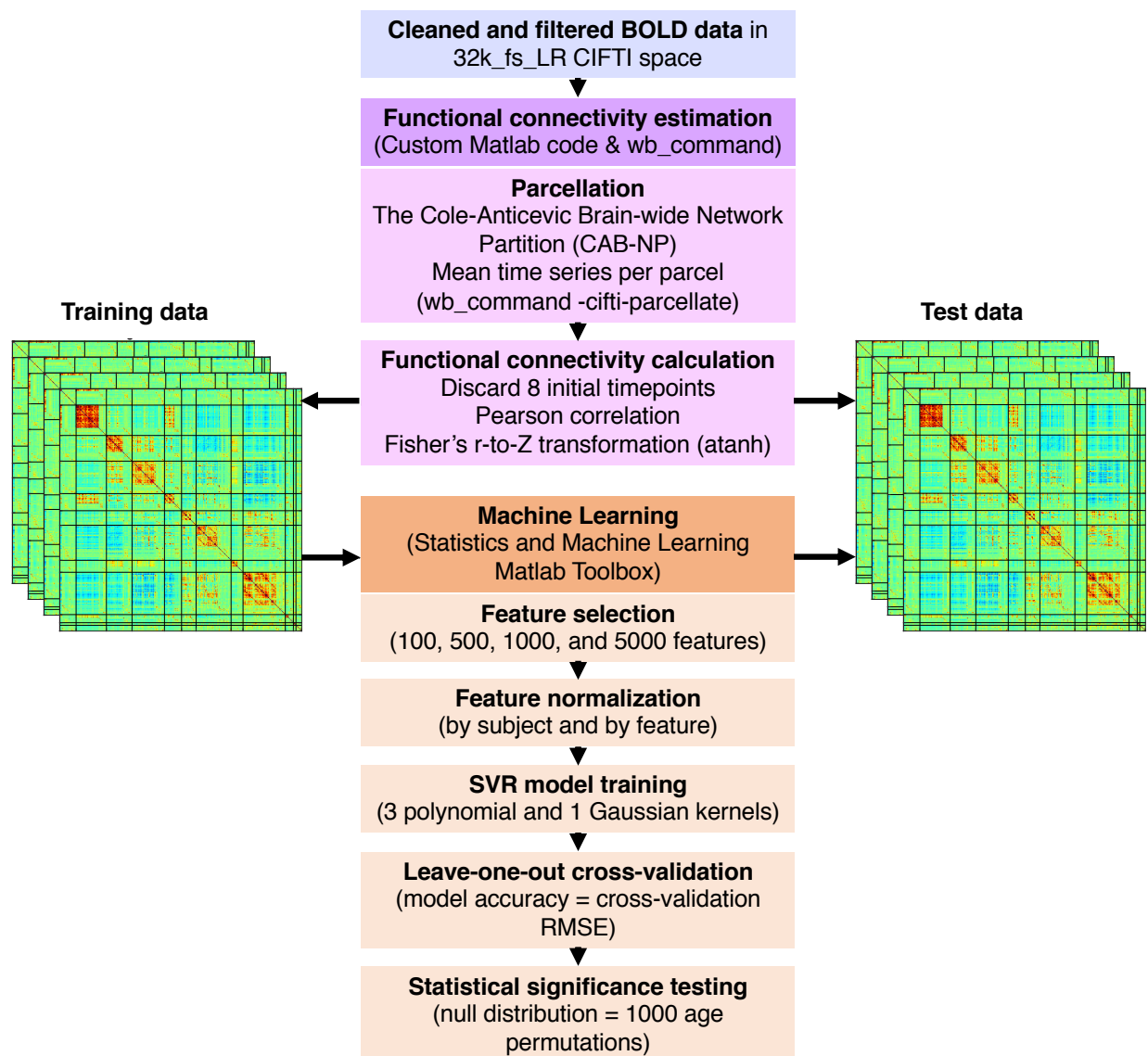
Figure S8. Overview of the functional connectivity estimation and machine learning workflows.

We trained several machine learning algorithms on the training dataset using different numbers of features (i.e., edges or functional connections) and selected the model that had the lowest leave-one-out cross-validation prediction error (see Table S1 for prediction accuracy of different models). We combined the cingulo-opercular and orbito-affective networks into a single network cluster ("affective networks") and trained a normative model of affective network maturation by selecting features from that network cluster.

Feature selection. We trained the affective network functional maturation model on 100, 500, 1000, and 5000 features that showed the strongest absolute correlation with age. Features that were correlated with head motion were excluded. We used leave-one-out cross-validation to determine the optimal number of features based on the lowest cross-validation root-mean-square error (RMSE). Features were normalized within each participant (i.e., converted to z-scores) and then normalized by the mean and standard deviation of the training dataset (i.e., for each feature, we subtracted the group mean and divided by the group standard deviation).

Support vector regression. We used support vector regression (SVR; Drucker et al., 1997; Smola and Schölkopf, 2004; Vapnik, 1995) to train the normative model of affective network functional maturity using the four sets of selected features. SVR is a machine learning algorithm that represents each participant's functional connectivity matrix as a point in multidimensional space (i.e., hyperspace) and fits a linear model to the data in hyperspace. SVR is well-suited for high-dimensional data, such the functional connectome, which consists of over 100,000 unique connections. In contrast to multiple regression, SVR capitalizes on the rich and complex information contained in the functional connectome matrix without running the risk of multicollinearity and loss of degrees of freedom. We used linear epsilon-insensitive SVR implemented in Matlab's Statistics and Machine Learning Toolbox.

The performance of the SVR model can be controlled by two main parameters: epsilon and the C-parameter (e.g., Smola and Schölkopf, 2004). Epsilon defines the size of a tube around the regression line in hyperspace, within which data points that deviate from the regression line carry no penalty. The C-parameter controls the penalty imposed on data points outside of the epsilon-defined tube and helps to prevent overfitting. Thus, the C-parameter defines the trade-off between the flatness of the regression line and tolerance of data points that deviate from it beyond the epsilon margin, such that a larger C allows for a steeper regression line. The loss function is estimated based on each data point's deviation from the epsilon-defined boundary. Smaller epsilon and larger C result in a more flexible model, which is more susceptible to overfitting.

Given that SVR fits a linear model in hyperspace, non-linear relationships between predictor and outcome variables can be tested using the "kernel trick", which transforms nonlinear input data into a higher-dimension feature space, where a linear model can be fitted (e.g., Ben-Hur et al., 2008). Commonly used kernels include polynomial kernels and Gaussian kernels, where the polynomial degree and the sigma control the flexibility of the two kernels, respectively. A larger polynomial degree and smaller sigma are associated with higher risk of overfitting (e.g., Ben-Hur et al., 2008). We trained four SVR models using four different kernels: linear kernel SVR, quadratic kernel SVR, cubic kernel SVR, and Gaussian kernel SVR (sigma = 130). For all the SVR models, we used the following parameters: epsilon = 1.45, C-parameter = 14.5, which were determined using a heuristic procedure in Matlab and yielded optimal performance.

To determine the accuracy of each SVR model trained on four different sets of features (100, 500, 1000, and 5000), we performed leave-one-out cross-validation (LOOCV). Each participant was excluded from the training sample one at a time, and the model was trained on the remaining participants. The held-out participant was then used to test the model. This

procedure was repeated for each participant in the training dataset. In selecting the best performing model, we used the following criteria: lowest LOOCV RMSE, largest LOOCV R^2, lowest number of features, and simplest kernel. Optimal prediction accuracy was achieved with the linear kernel SVR trained on 500 features (see Table S1).

  Significance testing of model accuracy. To determine whether the predictive performance of the selected model was statistically different from chance, we used permutation testing. We generated the null distribution by randomly permuting age labels of the training dataset 1000 times and re-trained the model on the permuted data. The statistical significance of the model was determined as the proportion of times a permuted model generated a cross-validation RMSE less than or equal to that of a model trained on true age labels. The selected linear kernel SVR model trained on 500 features was statistically significant at $p < 0.001$.

  Control models. Given that head motion is associated with both age and functional connectivity, we tested whether the SVR model's performance was driven by age-related differences in head motion. We trained the SVR model to predict individual framewise displacement (FD) using the same parameters and features as were used to predict age. We then tested the statistical significance of the FD-predicting model using 1000 permutations to build the null distribution. The model trained to predict FD was not statistically significant (RMSE = 0.11, R^2 = 0.21, p = 0.99), suggesting that the predictive performance of the age-predicting model of functional brain maturation was not driven by age-related differences in head motion.

  Table S1. Cross-validation root-mean-square errors (RMSE) and R^2 for each of the trained models. The model that was selected as the final normative model is highlighted with a box.

Functional maturity model	Number of selected features			
RMSE	**100**	**500**	**1000**	**5000**
Linear kernel SVR	5.06	**4.56**	4.77	5.57
Quadratic kernel SVR	5.18	4.64	4.86	5.84
Cubic kernel SVR	5.37	4.91	5.16	6.29
Gaussian kernel SVR	11.1	7.98	6.8	6.42
R^2	**100**	**500**	**1000**	**5000**
Linear kernel SVR	0.81	**0.86**	0.85	0.82
Quadratic kernel SVR	0.81	0.86	0.85	0.81
Cubic kernel SVR	0.8	0.85	0.85	0.81
Gaussian kernel SVR	0.59	0.82	0.82	0.8

Orbito-Affective
Ventral Multimodal
Posterior Multimodal

Default Mode

Auditory

Frontoparietal

Language

Dorsal Attention

Cingulo-Opercular
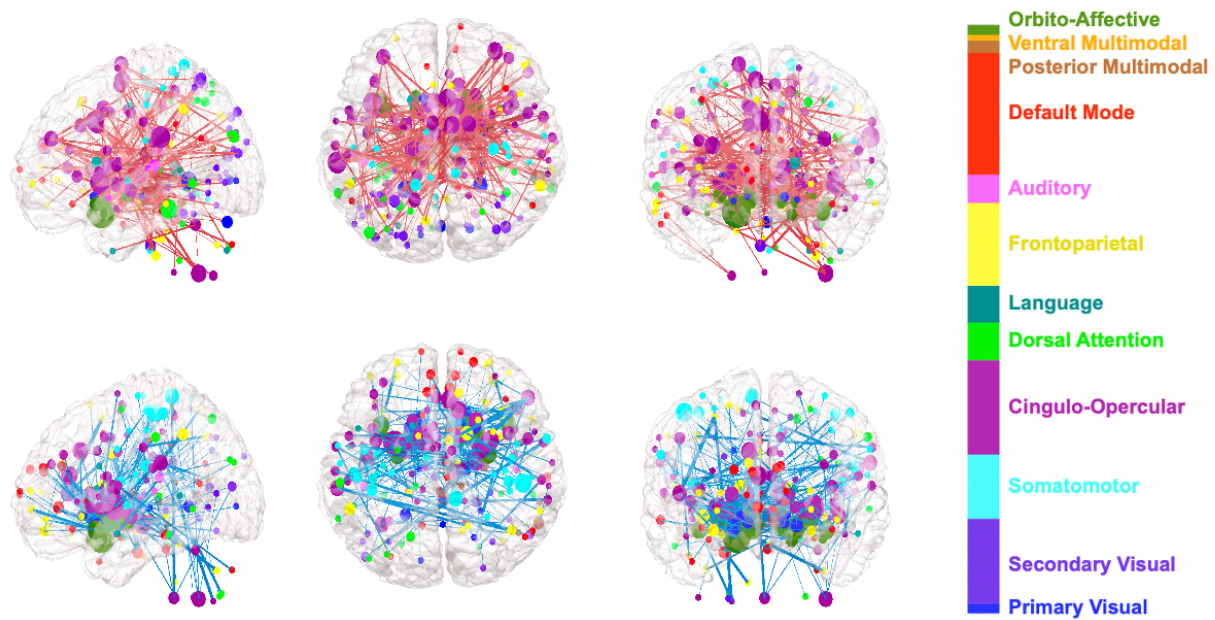
Somatomotor

Secondary Visual

Primary Visual

Figure S9. Functional connections with the greatest positive (top panel) and negative (bottom panel) SVR weights (n = 500). Lines represent functional connections (i.e., red lines = positive edges; blue lines = negative edges). Line width is proportional to absolute SVR weights. Circles represent ROIs. Circle size is proportional to the number of positive or negative edges a given ROI forms. Circle color denotes one of the 12 CAB-NP functional networks.
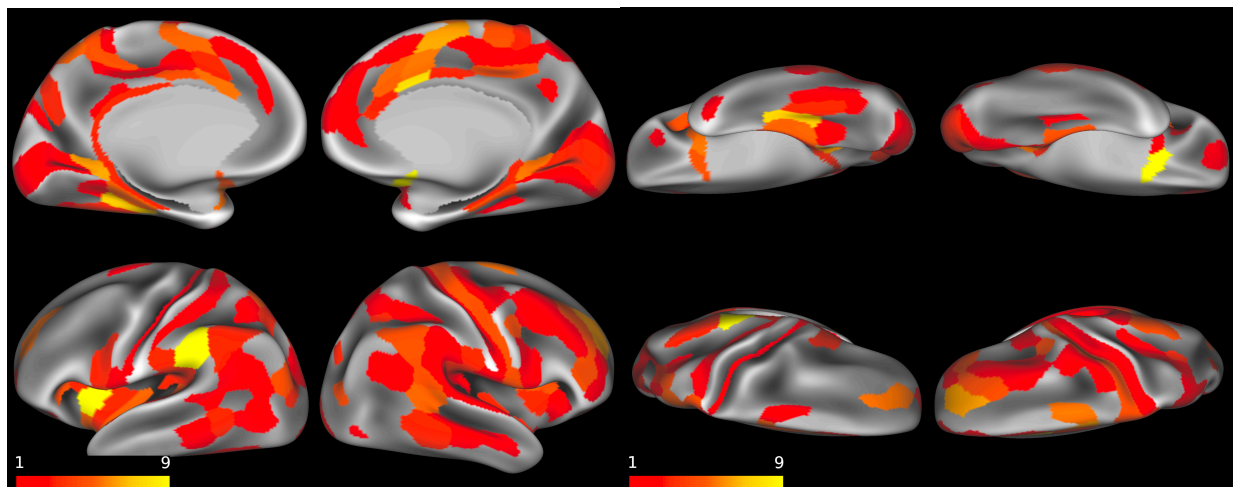

Figure S10. ROIs whose connectivity with other ROIs was positively associated with age. Color denotes number of positive edges a given ROI makes.
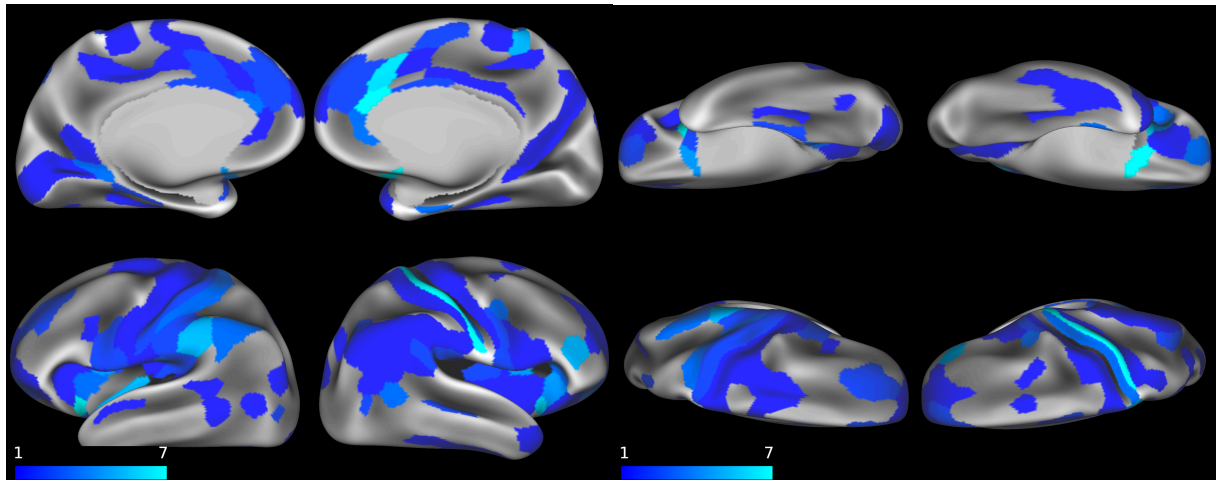
Figure S11. ROIs whose connectivity with other ROIs was negatively associated with age. Color denotes number of negative edges a given ROI makes.

References

Avants, B. B., Epstein, C. L., Grossman, M., & Gee, J. C. (2008). Symmetric diffeomorphic image registration with cross-correlation: Evaluating automated labeling of elderly and neurodegenerative brain. *Medical Image Analysis, 12*(1), 26-41. https://doi.org/10.1016/j.media.2007.06.004

Ben-Hur, A., Ong, C. S., Sonnenburg, S., Schölkopf, B., & Rätsch, G. (2008). Support vector machines and kernels for computational biology. *PLoS Computational Biology, 4*(10), 1-10. https://doi.org/10.1371/journal.pcbi.1000173

Burgess, G. C., Kandala, S., Nolan, D., Laumann, T. O., Power, J. D., Adeyemo, B., ... & Barch, D. M. (2016). Evaluation of denoising strategies to address motion-correlated artifacts in resting-state functional magnetic resonance imaging data from the human connectome project. *Brain Connectivity, 6*(9), 669-680. https://doi.org/10.1089/brain.2016.0435

Ciric, R., Wolf, D. H., Power, J. D., Roalf, D. R., Baum, G. L., Ruparel, K., ... & Gur, R. C. (2017). Benchmarking of participant-level confound regression strategies for the control of motion artifact in studies of functional connectivity. *NeuroImage, 154*, 174-187. https://doi.org/10.1016/j.neuroimage.2017.03.020

Coalson, T. S., Van Essen, D. C., & Glasser, M. F. (2018). The impact of traditional neuroimaging methods on the spatial localization of cortical areas. *Proceedings of the National Academy of Sciences, 115*(27), E6356-E6365. https://doi.org/10.1073/pnas.1801582115

Dale, A. M., Fischl, B., & Sereno, M. I. (1999). Cortical surface-based analysis: I. Segmentation and surface reconstruction. *NeuroImage, 9*(2), 179-194. https://doi.org/10.1006/nimg.1998.0395

Dickie, E. W., Anticevic, A., Smith, D. E., Coalson, T. S., Manogaran, M., Calarco, N., ... & Voineskos, A. N. (2019). Ciftify: A framework for surface-based analysis of legacy MR acquisitions. *NeuroImage, 197*, 818-826. https://doi.org/10.1016/j.neuroimage.2019.04.078

Drucker, H., Burges, C. J., Kaufman, L., Smola, A. J., & Vapnik, V. (1997). Support vector regression machines. In *Advances in Neural Information Processing Systems* (pp. 155-161).

Esteban, O., Markiewicz, C. J., Blair, R. W., Moodie, C. A., Isik, A. I., Erramuzpe, A., ... & Oya, H. (2019). fMRIPrep: A robust preprocessing pipeline for functional MRI. *Nature Methods, 16*(1), 111-116. https://doi.org/10.1038/s41592-018-0235-4

Fonov, V. S., Evans, A. C., McKinstry, R. C., Almli, C. R., & Collins, D. L. (2009). Unbiased nonlinear average age-appropriate brain templates from birth to adulthood. *NeuroImage, 47*, S102. https://doi.org/10.1016/S1053-8119(09)70884-5

Glasser, M. F., Coalson, T. S., Robinson, E. C., Hacker, C. D., Harwell, J., Yacoub, E., ... & Smith, S. M. (2016). A multi-modal parcellation of human cerebral cortex. *Nature, 536*, 171-178. https://doi.org/10.1038/nature18933

Glasser, M. F., Sotiropoulos, S. N., Wilson, J. A., Coalson, T. S., Fischl, B., Andersson, J. L., ... & Van Essen, D. C. (2013). The minimal preprocessing pipelines for the Human Connectome Project. *NeuroImage, 80*, 105-124. https://doi.org/10.1016/j.neuroimage.2013.04.127

Gorgolewski, K., Burns, C. D., Madison, C., Clark, D., Halchenko, Y. O., Waskom, M. L., & Ghosh, S. S. (2011). Nipype: A flexible, lightweight and extensible neuroimaging data processing framework in python. *Frontiers in Neuroinformatics, 5*, 13. https://doi.org/10.3389/fninf.2011.00013

Greve, D. N., & Fischl, B. (2009). Accurate and robust brain image alignment using boundary-based registration. *NeuroImage, 48*(1), 63-72. https://doi.org/10.1016/j.neuroimage.2009.06.060

Huntenburg, J. M. (2014). *Evaluating nonlinear coregistration of BOLD EPI and T1w images* [Doctoral dissertation, Freie Universität Berlin]. Available from: http://hdl.handle.net/11858/00-001M-0000-002B-1CB5-A.

Jenkinson, M., Bannister, P., Brady, M., & Smith, S. (2002). Improved optimization for the robust and accurate linear registration and motion correction of brain images. *NeuroImage, 17*(2), 825-841. https://doi.org/10.1006/nimg.2002.1132

Ji, J. L., Spronk, M., Kulkarni, K., Repovš, G., Anticevic, A., & Cole, M. W. (2019). Mapping the human brain's cortical-subcortical functional network organization. *NeuroImage, 185*, 35-57. https://doi.org/10.1016/j.neuroimage.2018.10.006

Klein, A., Ghosh, S. S., Bao, F. S., Giard, J., Häme, Y., Stavsky, E., ... & Keshavan, A. (2017). Mindboggling morphometry of human brains. *PLoS Computational Biology, 13*(2). https://doi.org/10.1371/journal.pcbi.1005350

Lanczos, C. (1964). Evaluation of noisy data. *Journal of the Society for Industrial and Applied Mathematics, Series B: Numerical Analysis, 1*(1), 76-85. https://doi.org/10.1137/0701007

Parkes, L., Fulcher, B., Yücel, M., & Fornito, A. (2018). An evaluation of the efficacy, reliability, and sensitivity of motion correction strategies for resting-state functional MRI. *NeuroImage, 171*, 415-436. https://doi.org/10.1016/j.neuroimage.2017.12.073

Power, J. D., Barnes, K. A., Snyder, A. Z., Schlaggar, B. L., & Petersen, S. E. (2012). Spurious but systematic correlations in functional connectivity MRI networks arise from subject motion. *NeuroImage, 59*(3), 2142-2154. https://doi.org/10.1016/j.neuroimage.2011.10.018

Power, J. D., Mitra, A., Laumann, T. O., Snyder, A. Z., Schlaggar, B. L., & Petersen, S. E. (2014). Methods to detect, characterize, and remove motion artifact in resting state fMRI. *NeuroImage, 84,* 320-341. https://doi.org/10.1016/j.neuroimage.2013.08.048

Robinson, E. C., Garcia, K., Glasser, M. F., Chen, Z., Coalson, T. S., Makropoulos, A., ... & Hutter, J. (2018). Multimodal surface matching with higher-order smoothness constraints. *NeuroImage, 167*, 453-465. https://doi.org/10.1016/j.neuroimage.2017.10.037

Satterthwaite, T. D., Elliott, M. A., Gerraty, R. T., Ruparel, K., Loughead, J., Calkins, M. E., ... & Wolf, D. H. (2013a). An improved framework for confound regression and filtering for control of motion artifact in the preprocessing of resting-state functional connectivity data. *NeuroImage, 64*, 240-256. https://doi.org/10.1016/j.neuroimage.2012.08.052

Smola, A. J., & Schölkopf, B. (2004). A tutorial on support vector regression. *Statistics and Computing, 14*(3), 199-222. https://doi.org/10.1023/B:STCO.0000035301.49549.88

Smyser, C. D., Inder, T. E., Shimony, J. S., Hill, J. E., Degnan, A. J., Snyder, A. Z., & Neil, J. J. (2010). Longitudinal analysis of neural network development in preterm infants. *Cerebral Cortex, 20*(12), 2852-2862. https://doi.org/10.1093/cercor/bhq035

Treiber, J. M., White, N. S., Steed, T. C., Bartsch, H., Holland, D., Farid, N., ... & Chen, C. C. (2016). Characterization and correction of geometric distortions in 814 diffusion weighted images. *PloS One, 11*(3), e0152472. https://doi.org/10.1371/journal.pone.0152472

Tustison, N. J., Avants, B. B., Cook, P. A., Zheng, Y., Egan, A., Yushkevich, P. A., & Gee, J. C. (2010). N4ITK: Improved N3 bias correction. *IEEE Transactions on Medical Imaging, 29*(6), 1310-1320. https://doi.org/10.1109/TMI.2010.2046908

Vapnik, V. N. (1995). The nature of statistical learning theory. Springer, New York, 1995.

Zhang, Y., Brady, M., & Smith, S. (2001). Segmentation of brain MR images through a hidden Markov random field model and the expectation-maximization algorithm. *IEEE Transactions on Medical Imaging, 20*(1), 45-57. https://doi.org/10.1109/42.906424